NASA CONTRACTOR REPORT

NASA CR-2664

NASA CR-2664

A STUDY OF METEOR SPECTROSCOPY AND PHYSICS FROM EARTH-ORBIT: A PRELIMINARY SURVEY INTO ULTRAVIOLET METEOR SPECTRA

David D. Meisel

Prepared by
STATE UNIVERSITY OF NEW YORK
Geneseo, N. Y. 14454
for Langley Research Center

NATIONAL AERONAUTICS AND SPACE ADMINISTRATION • WASHINGTON, D. C. • APRIL 1976

1. Report No.	2. Government Accession No.	3. Recipient's Catalog No.
NASA CR-2664		

4. Title and Subtitle	5. Report Date
A Study of Meteor Spectroscopy and Physics from Earth-Orbit: A Preliminary Survey into Ultraviolet Meteor Spectra	April 1976
	6. Performing Organization Code

7. Author(s)	8. Performing Organization Report No.
David D. Meisel	
	10. Work Unit No.

9. Performing Organization Name and Address	11. Contract or Grant No.
Department of Physics and Astronomy State University of New York Geneseo, New York 14454	L-13631A
	13. Type of Report and Period Covered
12. Sponsoring Agency Name and Address	Contractor Report
National Aeronautics and Space Administration Washington, DC 20546	14. Sponsoring Agency Code

15. Supplementary Notes

Technical monitor: Gale A. Harvey, Langley Research Center

Final report

16. Abstract

Preliminary data required to extrapolate available meteor physics information (obtained in the photographic, visual and near ultraviolet spectral regions) into the middle and far ultraviolet are presented. Wavelength tables, telluric attenuation factors, meteor rates, and telluric airglow data are summarized in the context of near-Earth observation vehicle parameters using moderate to low spectral resolution instrumentation. Considerable attention is given to the problem of meteor excitation temperatures since these are required to predict the strength of UV features. Relative line intensities are computed for an assumed chondritic composition. Features of greatest predicted intensities, the major problems in meteor physics, detectability of UV meteor events, complications of spacecraft motion, and UV instrumentation options are summarized with recommendations for future work.

17. Key Words (Suggested by Author(s)) (STAR category underlined)	18. Distribution Statement
Ultraviolet Meteor Spectroscopy Light Element Abundances	Unclassified - Unlimited Subject Category 89

19. Security Classif. (of this report)	20. Security Classif. (of this page)	21. No. of Pages	22. Price*
Unclassified	Unclassified	82	$4.75

For sale by the National Technical Information Service, Springfield, Virginia 22161

Table of Contents

Tables

Tables (continued)

Introduction

Significant libraries of photographic meteor spectra now exist particularly at NASA Langley Research Center and are being studied to better understand meteor processes and to yield meteoroid elemental abundances. However, virtually all of these spectra cover only the 3400-6800 Å interval and cannot provide abundances of the lighter elements such as hydrogen or carbon. It is the lighter elements that are of considerable cosmogonical importance especially with regard to the chemical origin of meteoroids, cosmic dust, and their supposed progenitors--the comets. This report represents a preliminary study of the feasibility of obtaining light element information from the ultraviolet spectra of meteors.

In a search of the literature as well as some original spacecraft records, no *direct* evidence of ultraviolet meteor events could be found, particularly for wavelengths below 3000 Å. Indirect evidence for strong ultraviolet emission has been proposed by McKinley and Millman (1949), Cook and Hawkins (1960), and by Rajchl (1969) in connection with the meteoric head-echo problem of radar returns from meteor trails (McIntosh, 1961, 1962, and 1963; McKinley, 1955). The interpretation on the basis of photoionization, however, requires an unusually high value of the ionic recombination coefficient. In addition, there is a definite solar modulation of the head-echo phenomenon that is difficult to reconcile with a simple photoionization event. With the exception of a very recent experiment by Harvey (1975) in which three meteors were detected photoelectrically in the 150 Å around 3090 Å from a high altitude (3250 meters) ground-based station, no positive evidence for natural meteoric UV emission (λ < 3300 Å) could be obtained.

Artificial meteor results (Tagliaferri and Slattery, 1969) down to 2400 Å indicate that for slow meteors ($\sim$30 km/sec) the UV spectrum peaks at 3700 Å with a secondary peak of about 1/3 of the 3700 Å intensity at 2900 Å. At 2400 Å the spectrum rises to a value 1/2 that of the 3700 Å peak. Some uncertainty was attached to the 2400 Å value because of instrumental characteristics so that a UV enhancement is not substantiated. Insufficient spectral resolution renders these results unsuitable for present extrapolation purposes.

Because of the relatively short time available, it was therefore necessary to use preliminary information derived from relatively few photographic spectra and attempt a gross extrapolation into the ultraviolet part of the spectrum. This extrapolation as will be noted later in this report, somewhat blindly leaps over important questions of meteor physics that remain to be clarified by careful examination at a later date. A number of *ad hoc* assumptions have been made at several critical points in the somewhat lengthy discussion that follows and it is hoped that my colleagues will recognize the necessarily hypothetical framework in which the extrapolation is cast and *not* interpret the present effort as a formal scientific theory of meteor excitation and ionization. It is rather an initial engineering study designed to enable educated guesses to be made in an area where no direct quantitative information is readily available. If the phenomenology of the ultraviolet meteor spectrum is not significantly different from the photographic spectrum, the proposed extrapolations should be satisfactory for planning future UV meteor experiments both from spacecraft and the ground. Formulation of a theory of meteor physics which will confirm or refute the chosen extrapolation process may well have to await the results of future direct UV detection experiments themselves.

References - Introduction

1. Cook, A. F.; and Hawkins, G. S.: The Meteoric Head Echo. Smithsonian Contr. Astrophys., vol. 5, 1960, pp. 1-7.

2. Harvey, G. A.: Ultraviolet Hydroxyl Observations of Perseid Meteors. Astrophys. J. Letters, 1975.

3. McIntosh, B. A.: Analysis of a Type of Rough-Trail Meteor Echo. Canadian J. Phys., vol. 39, 1961, pp. 437-444.

4. _____: The Meteoric Head Echo. J. Atm. and Terr. Phys., vol. 24, 1962, pp. 311-315.

5. _____: Experimental Study of the Amplitude of Radar Meteor-Head Echos. Canadian J. Phys., vol. 41, pp. 355-371.

6. McKinley, D. W. R.; and Millman, P. M.: A Phenomenological Theory of Radar Echoes from Meteors. Proc. IRE, vol. 37, 1949, pp. 364-375.

7. Rajchl, J.: On the Interaction Layer in Front of a Meteor Body. Bull. Astron. Inst. Czech., vol. 20, 1969, pp. 363-372.

8. Tagliaferri, E.; and Slattery, J. C.: A Spectral Measurement of Simulated Meteors. Astrophys. J., vol. 155, 1969, pp. 1123-1127.

Part I - Preliminary Data

In this part of the report, several miscellaneous items relating to the ultraviolet meteor detection problem are presented mainly in tabular form.

A. Wavelength Information and Lists.

First, in Tables I, II, and III the strongest and most likely ultraviolet meteor emission features, particularly those with $\lambda < 2000$, for each element and molecule are listed along with possible interfering or blending features which may be bothersome at low dispersion. In Part III of this report, calculations relating to the likely visibility of certain features selected from these lists will be presented. In these lists the following abbreviations for common molecular bands are used:

Molecular Abbreviations

O_2 SR = Schumann Runge O_2 B $^3\Sigma_u^- \overset{\leftarrow}{\rightarrow} X\ ^3\Sigma_g^-$

N_2 VK = Vegard-Kaplan A $^3\Sigma_u^+ \overset{\leftarrow}{\rightarrow} X\ ^1\Sigma_g^+$

N_2 OTW = Ogawa-Tanaka-Wilkinson $B^1\ ^3\Sigma_u^- \leftarrow X\ ^1\Sigma_g^+$

N_2 OTWM = Ogawa-Tanaka-Wilkinson-Mulliken $a^1\ ^1\Sigma_u^- \overset{\leftarrow}{\rightarrow} X\ ^1\Sigma_g^+$

N_2 LBH = Lyman-Birge-Hopfield a $^1\pi_g \overset{\leftarrow}{\rightarrow} X\ ^1\Sigma_g^+$

Selection of likely molecular species represent only suggestions based on an assumed carbonaceous chondritic composition for meteoroids. The only molecular species so far (July 1975) definitely observed in meteor spectra are due to air radiation.

Table I - Strong UV Lines, Atomic Species

Species	λ_{vac} (or λ_{air})*	Possible Interference at Low Dispersion
H I	1215.67 Å	N I 1199-1201, N_2 OTW(0-12)
Be I	2348.61	Fe II 2348, 2344, 2343, 2359 Co I 2358, N_2 LBH(7-18)
B I	2497.72	Fe I 2501, O_2 SR(2-7)
	2496.77	O_2 SR(2-7)
	1826.40	S I 1826, Mg I λ1828, N_2 LBH(1-7)
C I	1658.12	N_2 LBH(3-6)
	1657.91	
	1657.38	
	1657.01	
	1656.93	
	1656.27	
N I	1200.71	Ly α, Atm. N I, O_2 Abs. Edge N_2 OTW(0-13)
	1200.22	
	1199.55	
O I	1306.03	S I 1305.88, Atm. O I
	1304.86	P II, Si II 1304.37
	1302.17	S I 1302-1303
[O I]	2972.3	Fe I 2970, 2973, 2949, 2953
	2958	
Na I	2852.81	weak transition (not likely to be observed)
	2853.01	
Mg I	2852.13	Na I 2852-53
	2025.84	Co II 2022, 2026, 2027, O_2 SR(0-0) N_2 LBH(4-12) (5-2) (11-4)

*λ_{air} given when $\lambda > 2000$ Å

Table I (continued)

Species	λ_{vac} (or λ_{air})*	Possible Interference at Low Dispersion
Al I	3092.84 Å	Co I 3110-3121
	3092.71	
	3082.15	Co I 3086
	2575.10	Mn II 2576
	2567.98	Fe I 2549
	2373.12	Mn I 2372, Fe II 2374
Si I	2528.51	Fe I 2527, 2529, 2535, N_2 LBH(11-23)
	2524.11	Fe I 2524, 2522, O_2 SR(1-7)
	2516.11	Fe I 2518, 2510
P I	1787.68	Ni II 1788, O_2 SR(14-0), N_2 LBH(3-8):
	1782.87	O_2 SR(13-0)
	1774.99	Ni II 1774, O_2 SR(12-0)
	1679.71	
	1674.61	
	1671.68	Al II 1671, N_2 LBH(2-7)
	1826.26	Mg I 1828, O_2 SR(14-1)
	1820.36	B I 1826, Si II 1817, O_2 SR(15-1), N_2 LBH(1-7)::
	1807.34	Si II 1808, N_2 LBH(0-6)
	1483.04	
	1474.00	
Ca I	2721.64	Fe I 2719, 2720, 2723, N_2 VK(5-9):
Ti I	3653.50	Co I 3653
	3642.67	Ni I 3642
	3635.46	Co I 3631
	3371.45	Ni I 3370
	3354.63	N_2 VK(0-9)
	3341.88	
V I	3226.11	
	3217.12	
	3207.41	
	3202.38	N_2 VK(1-9)
	3198.01	
	3185.40	
	3183.98	
	3183.96	
	3183.41	
Cr I	3605.33	Ni I 3610, Co I 3602, N_2 VK(0-10)
	3593.48	Co I 3594, Si II 3590
	3578.68	Si II 3580, 3576, N_2 VK(3-12)

*λ_{air} given when $\lambda > 2000$ Å

Table I (continued)

Species	λ_{vac} (or λ_{air})*	Possible Interference at Low Dispersion
Mn I	2801.08 Å	Mg II 2802.7
	2798.27	Two weak N_2 systems
	2794.82	Mg II 2795.5
Fe I	3440.61	
	3059.09	Ti II 3060, 3057
	3047.60	Co I 3049, 3044
	3037.39	
	3025.84	
	3021.07	
	3020.64	
	3020.49	Co I 3017.5
	3008.14	
	3000.95	N_2 VK(1-8)
	2994.43	
	2983.57	Co I 2987
	2973.24	
	2973.13	
	2970.11	
	2966.90	
	2965.26	
	2957.36	
	2953.94	
	2948.88	
	2936.90	N_2 VK(0-7)
	2750.14	V II 2747.75
	2744.07	V II 2742.43
	2737.31	V II 2740, 2741, Li I 2741
	2723.58	V II 2729, 2723
	2720.90	Ca I 2721.6
	2719.03	V II 2715
	2549.61	
	2545.98	
	2540.97	
	2535.60	
	2529.13	Si I 2528
	2527.43	
	2524.29	Si I 2524, N_2 VK(4-7)
	2522.85	
	2518.10	Si I 2519.2
	2510.83	Si I 2514, 2516, N_2 VK(1-5)
	2501.13	Si 2506
	2491.16	
	2490.64	
	2489.75	

*λ_{air} given when λ > 2000 Å

Table I (continued)

Species	λ_{vac} (or λ_{air})*	Possible Interference at Low Dispersion
Fe I (cont.)	2488.14 Å	
	2484.19	
	2483.27	
	2479.78	Ti II 2478, 2474, N_2 VK(4-5)
	2472.91	N_2 VK(8-9)
	2462.64	
	2631.32	
Co I	3575.36	Si II 3576, 3572
	3526.85	Ni I 3524, 3519
	3072.34	Ti II 3072
	3061.82	Ti II 3066, 3059, Fe I 3059
	3044.00	Fe I 3048, 3037
	(Also numerous lines between 2335-2415), some N_2 VK possible	
Ni I	3391.05	Ti II 3394, 3387
	3500.85	Fe I 3497
	3369.57	Ti I 3371
	3610.46	Cr I 3605
	3597.70	Co I 3602, 3594
	3524.54	Fe I 3526, Co I 3520
	3510.34	
	3492.96	Fe I 3498, 3490
	3515.05	Co I 3520
	3458.47	Fe I 3443
	3414.76	
Cu I	3273.96	Ni I 3287, Ti II 3252, 3254
	3247.54	Ti II 3252, 3242
Zn I	2138.56	
	1589.76	C I 1561, 1598

*λ_{air} given when λ > 2000 Å

References

1. Morton, D. C. and Smith, W. H. 1973 Ap. J. Suppl. No. 26, pp. 333-364.

2. Moore, C. E. 1945 Contr. Princeton Univ. Obs. No. 20.
   ———————. NBS Circ. 467, Sections 1, 2, 3 1949, 1952, 1958.
   ———————. NBS Circ. 488, Sections 1-5 1950, 1952, 1962.
   ———————. NSRDS-NBS 3, Sections 1-6 1965-1972.
   ———————. NSRDS-NBS 34.

3. Rosen, B. Spectroscopic Data Relevant to Diatomic Molecules, Vol. 17, Tables de Constants et Données Numériques 1970, Pergamon Press.

Table II - Strong UV Lines, Ionic Species

Species	λ_{vac} (or λ_{air})*	Possible Interference at Low Dispersion
Mg II	2802.70 Å 2795.53	Mn I 2798, 2794, 2801
Al II	1670.79	P I 1671, 1674, 1679, N_2 LBH(0-4) is near
Si II	1533.44	
	1526.72	N_2 LBH(5-5)
	1309.27	S I 1310
	1304.37	O I, S I, N_2 LBH(5-0)
	1265.02	N_2 LBH(8-1)
Ti II	3349.57	N_2 VK(0-9) nearly
	3361.21	
	3372.80	
	3380.28	
	3383.76	
	3387.83	
	3394.57	
	3217-3254	
	3066-3088	
Mn II	2605.70	O_2 SR(2-8), N_2 LBH(15-27)
	2593.73	N_2 VK(0-5)
	2576.11	Al I 2575 , N_2 VK(5-8)
Fe II	2631.04	Ti II 2631
	2628.29	
	2625.66	
	2617.62	Ti I 2619, N_2 VK(3-7)
	Also 2327-2631	Numerous weak lines, N_2 VK
Zn II	2062.02	Cr II 2061, Co II 2064, N_2 LBH(6-14)
	2025.51	Mg I 2026, Co II 2027, 2025, 2022, N_2 LBH(4-12)

*λ_{air} given when $\lambda > 2000$ Å

References

1. Morton, D. C. and Smith, W. H. 1973 Ap. J. Suppl. No. 26, pp. 333-364.

2. Moore, C. E. 1945 Contr. Princeton Univ. Obs. No. 20.
   _____. NBS Circ. 467, Sections 1, 2, 3 1949, 1952, 1958.
   _____. NBS Circ. 488, Sections 1-5 1950, 1952, 1962.
   _____. NSRDS-NBS 3, Sections 1-6 1965-1972.
   _____. NSRDS-NBS 34.

3. Rosen, B. Spectroscopic Data Relevant to Diatomic Molecules, Vol. 17, Tables de Constants et Données Numériques 1970, Pergamon Press.

Table III - Additional Possible UV Features

A. Atomic and Ionic Species (Wavelengths in Angström Units)

H I	1025.72, 972.54
C I	1561.44, 1329.58, 1277.55, 1277.28, 1261.55
C II	1335.71, 1037.02
N II	1085.70, 1084.58, 916.70
O I	1355.60, 1039.23
Al I	1936.44, 1931.92
Si I	2506.90, 2216.67, 2210.89, 1988.99, 1850.67, 1847.47, 1258.79, 1256.49
Si II	1264.73, 1260.42, 1197.39, 1194.50, 1193.28, 1190.42, 1023.69
P II	1310.70, 1159.08, 1155.00, 1149.96
S I	1826.26, 1820.36, 1807.34, 1483.036, 1474.00, 1433.33, 1425.06, 1316.57, 1302.34, 1296.17, 1295.66
S II	1259.52, 1253.81
Ca II	1651.99, 1649.86, 1342.55, 1341.8, 1227.03, 1226.73
Ti III	1298.95, 1298.67, 1295.91, 1294.67, 1291.64, 1289.32, 1286.38
V II	2700.94, 2687.96
Mn II	2605.697, 2593.73, 1201.12, 1199.39, 1197.17
Fe II	2599.40, 2410.52, 2404.88, 2382.03, 2343.50, 1629.15, 1608.46
Co I	2411.62, 2407.25, 2380.48, 2365.06, 2605.54, 2025.76, 2022.36, 2011.55
Ni II	1751.92, 1741.56, 1454.96, 1370.20, 1317.75
Cu II	1358.76
Zn I	1457.57

References

1. Morton, D. C. & Smith, W. H. 1973, Ap. J. Suppl. No. 26, pp. 333-364.

2. Morton, D. C. 1975, Ap. J. 197, 85.

Table III (continued)

B. Some Possible Far UV Molecular Features

Species	Transition	Wavelengths
CO	$A\ ^1\Pi - X\ ^1\Sigma^+$	
	(0-3)	1447.36
	(0-4)	1419.04
	(0-5)	1392.53
	(0-6)	1367.62
	(0-7)	1344.18
	(0-8)	1322.15
	(0-9)	1301.40
	(0-10)	1281.87
$C^{13}O^{16}$	(0-5)	1395.3
	(0-6)	1370.7
CO	others	1076, 1088, 1150
OH	D - X	1221.17, 1222.07, 1222.52
SiO	J - X	1310.01
H_2O	$3p^1\tilde{B}_1 - X^1\tilde{A}_2$	1239.73, 1192.72
N_2 (Air)	VK, OTW, OTWM, and LBH Bands	
O_2 (Air)	SR Band	

References

1. Morton, D. C. and Smith, W. H. 1973 Ap. J. Suppl. No. 26, pp. 333-364.

2. Moore, C. E. 1945 Contr. Princeton Univ. Obs. No. 20.
_____. NBS Circ. 467, Sections 1, 2, 3 1949, 1952, 1958.
_____. NBS Circ. 488, Sections 1-5 1950, 1952, 1962.
_____. NSRDS-NBS 3, Sections 1-6 1965-1972.
_____. NSRDS-NBS 34.

3. Rosen, B. Spectroscopic Data Relevant to Diatomic Molecules, Vol. 17, Tables de Constants et Données Numériques 1970, Pergamon Press.

C. Possible Additional Molecular Species UV Meteor Spectra

Species	Transition	Band Origin Wavelength (Å)	Band Oscillator Strength
C_2	B-X	2512	?
CH	c-X	3145	0.008
OH	A-X	3086	0.0012
NO	A-X	2262, 2269	0.002
SiO	A-X	2345	?
AlO	B-X	3020	?

D. Possible Molecular Species in Near UV - Visible or IR Meteor Spectra

C_2	A-X	5160	0.029
	c-b	3851	0.06
CH	A-X	4310	0.006
CN	B-X	3876	0.029
NH	A-X	6443	0.002
AlO	A-X	4846	?
FeO	D-A	7750	?
	B-X	5791	?
	c-X	5615	?
	D-X	5584	?
	E-X	4479	

References

1. Allen, C. W. 1963, Astrophysical Quantities, 78, The Athlone Press, Univ. of London.

2. Herzberg, G. 1950, Spectra of Diatomic Molecules, D. Van Nostrand Co.

B. Atmospheric Attenuation.

For a spacecraft above 80 kilometers, calculation shows that Rayleigh scattering and ozone attenuation are not significant. For the wavelength range from the LiF cutoff (~1100Å) to 2000Å the O_2 Schumann-Runge bands can provide significant attenuation for objects located below 150 kilometers. In addition atmospheric O I, N I, and H I produce significant line absorption for meteoric lines of the same elements.

Calculations of the O_2, O I, N I, and H I attenuation between 95 kilometers and 200 kilometers have been carried out assuming that nighttime densities (at a sunspot number of 50 and above 100 kilometers) are equal to the daytime values at sunspot minimum. Atmospheric profiles for O_2, O I, and N I were taken from Johnson (1961) and H I densities were obtained from models calculated by Meier and Prinz (1970). Column densities obtained by numerical integration of the models from 95 km to 200 km were

For O I $\int N d\ell = 3.2 \times 10^{17}$ cm^{-2} For H I $\int N d\ell = 7.5 \times 10^{12}$ cm^{-2}

For N I $\int N d\ell = 1.3 \times 10^{16}$ cm^{-2} For O_2 $\int N d\ell = 4.9 \times 10^{18}$ cm^{-2}

As a check on the numerical integration of the models the atmospheric equivalent widths for Ly α (1216Å) of H I and for O I 1302, 1305, 1306 Å were calculated and compared to the unpublished data of Brueckner (Opal, 1975) using the CALROC rocket. In addition, the O_2 column density obtained above compares excellently with O_2 densities measured in the same CALROC experiment.

In the calculations of atmospheric attenuation all atmospheric atomic absorptions were assumed to be optically thick with Doppler profiles appropriate to an average temperature over the entire atmosphere between 95 km and 200 km. The following were taken as representative values.

Species	Doppler Half Intensity Half Width	T (°K)	Dimensionless Absorption Coefficient*
O I	2.5×10^{-3} Å	500°K	6.6×10^{5}
N I	2.7×10^{-3} Å	500°K	3×10^{4}
H I	1.0×10^{-2} Å	1000°K	47

*where $\zeta = \frac{\pi e^2}{mc} f \int \frac{N d\ell}{\alpha}$, $\alpha = \nu_o \left[\left(\frac{2kT}{mc^2}\right) \ln 2\right]^{1/2}$

as defined by Green and Wyatt (1965a)

where f = oscillator strength
N = density in cm^{-3}
α = Doppler half width
c = velocity of light
3 = electron charge
T = temperature
ν_o = frequency of line
m = electron mass
k = Boltzmann constant
ℓ = path length

The O_2 optical depth can be found directly (assuming O_2 is optically thick) using the absorption coefficients given by Cook and Metzger (1964)

$$\tau_{O_2} = 8.7 \times 10^{-11} \sqrt{k_\lambda (cm^{-1})} \left(\int_{l_1}^{l_2} n_{O_2} \, d\ell(cm) \right)^{1/2}$$

$(\Delta\lambda = 0.1 \text{ Å})$

For the atomic lines we assume that both the emission line and atmospheric absorption have Doppler profiles (Mitchell and Zemansky, 1961)

where

$$1 - e^{-\tau} = \frac{\int_{-\infty}^{+\infty} e^{-(\omega/\phi)^2} \left(1 - e^{-\zeta e^{-\omega^2}} \right) d\omega}{\int_{-\infty}^{+\infty} e^{-(\omega/\phi)^2} \, d\omega}$$

with τ = total line "optical depth," ζ as previously,

$$\phi = \sqrt{\frac{\text{T emission line}}{\text{T absorption line}}} \,,$$

$$\omega = \frac{(\nu - \nu_o)\sqrt{\ln 2}}{\alpha} \,,$$

α = the previously defined Doppler width,

and ν_o = the central frequency of the line.

As shown for Doppler profiles by Struve and Elvey (1934), thick absorbers have limiting equivalent widths given by

$$W = \frac{2\alpha}{(\ln 2)^{1/2}} \ln \left[\left(\frac{\ln 2}{\pi} \right)^{1/2} \zeta \right] \left[1 + \frac{0.57721}{2 \ln \left[(\ln 2/\pi)^{1/2} \zeta \right]} \right]$$

Comparison of the calculated equivalent widths and those observed shows

	W_{cal}	W_{obs}	Notes
O I	0.09 Å	0.09 Å	
H I	0.04	0.02	Low Solar Activity
		0.04	High Solar Activity

As demonstrated by Meier and Prinz (1970) the H I discrepancy is due to the isothermal assumption. Since we are interested in a somewhat pessimistic view (valid at moderately high solar activity) and only require accuracy ±0.1 in the logarithm, this is considered satisfactory agreement.

The results for O_2 attenuation which can be given down to 85 km with fair accuracy for a number of representative UV features are listed in Table IV. Since O_2 above 150 km is negligible it is possible to correct the calculations for detector to object distance by simply adding the appropriate logarithmic quantities from Table V. For example, suppose the intensity of the C I 1330 Å line is calculated to be 1.5×10^{-5} ergs/cm^2-sec for a meteor at 95 km as seen by a detector at 200 km. What is its intensity for the same conditions but for a detector at 250 km and a meteor at 100 km? From Table IV there will be a gain of $\log_{10}(I/I_o) = 0.31$ due to a decrease in O_2 attenuation. From Table V there is a distance loss of $\log_{10}(I/I_o) = -0.35$ for going out to 250 km but a gain of $\log_{10}(I/I_o) = 0.03$ for changing the meteor height from 95 km to 100 km. Thus the net change of intensity of $\log_{10}(I/I_o) = -0.01$. Thus moving the detector out to 250 km is nearly offset by changing meteor height from 95 km to 100 km.

The results for the atomic species attenuation is not as easily transformed and because the species densities below 95 km is unknown (Opal, private communication) it is not possible to carry the integrations below that height. However, since the atomic densities are likely to be small it seems reasonable to assume that the values will be approximately correct for meteors below 95 km also.

It should be remembered that the values quoted are only for daytime sunspot minimum and assumed to be valid nighttime near the middle of the sunspot cycle (spot number = 50).

At sunspot maximum, attenuations may be a factor of two or three higher and at sunspot minimum a factor of two or three lower than the values quoted.

Finally, it should be mentioned that it is not possible at this time to evaluate what the effects of possible hot O_2 and NO absorption in the immediate meteoroid environment will be on the observed intensity of far UV spectral lines. From considerations which will be discussed later, however, neither O_2 nor NO are expected to be a problem for meteors with geocentric velocities above 35 kilometers/sec.

Table IV - O_2 Absorption for Selected Possible Far UV Features in Meteor Spectra (Nighttime - middle of Solar Cycle or Daytime at Sunspot Minimum)

Species	λ	$\sqrt{k_\lambda}$ (cm^{-1})	Log_{10} Loss from 150 km (or above) down to 100 km	95 km	90 km	85 km
Unit Absorption Coeff. Loss			0.016	0.084	0.144	0.224
H I	1216A	0.2	0.003	0.017	0.029	0.045
	1025	5.4	0.086	0.454	0.778	1.21
	973	31.6	0.506	2.65	4.55	7.08
C I	1330	4.5	0.072	0.378	0.648	1.01
	1560-1660	20	0.320	1.68	2.88	4.48
C II	1037	5.5	0.088	0.462	0.792	1.23
	1335	4.5	0.072	0.378	0.648	1.01
N I	1200	3.2	0.051	0.269	0.461	0.72
N II	1085	5.5	0.088	0.462	0.792	1.23
O I	1357	10	0.160	0.840	1.44	2.24
	1304	3.2	0.051	0.269	0.461	0.72
	1040	7.7	0.123	0.647	1.11	1.72
O II	834	24.5	0.392	2.058	3.53	5.49
Al I	1931,1936*	0.3	0.004	0.025	0.043	0.07
Al II	1670	14.1	0.226	1.18	2.03	3.16
Si I	1255,56,58*	3.2	0.051	0.269	0.461	0.72
	1500-2000	20 to 0.3	0.32 to 0.0	1.68 to 0	2.88 to 0	4.48 to 0
Si II	1800	1.0	0.016	0.084	0.144	0.224 to 0
	1526,1533	15.8	0.253	1.33	2.27	3.54
	1304,1309	3.2	0.051	0.269	0.461	0.717
	1260,1265	1.4	0.022	0.118	0.202	0.314
	1190,94	3	0.048	0.252	0.432	0.672
	990-993	14.1	0.226	1.18	2.03	3.16
P I	1774-87	2.8	0.045	0.235	0.403	0.627
	1671-79	5.5	0.088	0.462	0.790	1.23
P II	1150-59	2.8	0.045	0.235	0.403	0.627
	1302-1310	4.5	0.072	0.378	0.648	1.01
	1532-1544	14.1	0.226	1.18	2.03	3.16
S I	1900,1914	0.32	0.005	0.027	0.046	0.072
	1807,20,26	1.00	0.016	0.084	0.144	0.224
	1300-1470	6.3	0.101	0.530	0.907	1.41
S II	1250,54,59	4.5	0.072	0.378	0.648	1.01
	906,910,912	17.3	0.277	1.45	2.49	3.87
Ca II	1649,1652	5.5	0.088	0.462	0.792	1.23
	1342	8.9	0.142	0.748	1.28	1.99
Ti III	1295-98	4.5	0.072	0.378	0.648	1.01
	1286-94	3.2	0.051	0.267	0.461	0.717

*Autoionization Lines

Table IV (continued)

Species	λ	$\sqrt{k_\lambda}$ (cm^{-1})	Log_{10} Loss from 150 km (or above) down to 100 km	95 km	90 km	85 km
Unit Absorption Coeff. Loss			0.016	0.084	0.144	0.224
V II	1570-2700	12.2 to 0.0	0.2 to 0.0	1.02 to 0.0	1.76 to 0.0	2.73
Mn II	1197,99,1201	8.9	0.142	0.747	1.28	1.99
Fe II	1260-75	5.5	0.088	0.462	0.792	1.23
	1600 group	10	0.16	0.840	1.44	2.24
	1848,58	0.7	0.011	0.059	0.101	0.157
Co II	1800-3000	1.0 to 0.0	0.016 to 0.0	0.08 to 0.0	0.144	0.224
Ni I	1900-3000	0.3 to 0.0	0.005 to 0.0	0.025 to 0.0	0.043	0.067
Ni II	1370,1393	10	0.160	0.840	1.44	2.24
Cu II	1359	10	0.160	0.840	1.44	2.24
Zn I	1458	17	0.277	1.45	2.49	3.88

To obtain stellar magnitudes multiply by 2.5

To obtain optical depth multiply by 2.3

For $\log_{10}(I/I_o)$ to 80 km use $\sqrt{k_\lambda}$ x 0.34

For $\log_{10}(I/I_o)$ to 75 km use $\sqrt{k_\lambda}$ x 0.52

Solar Cycle, Diurnal, and seasonal cycle variations are not expected to be over ±0.3 in the $\log_{10}(I/I_o)$ values.

Table V - Relative Distance Adjustments
for Different Detector Heights
and Different Meteor Heights

Meteor Height	Detector Height 200 km $\log_{10}(I/I_o)$	Detector Height 150 km $\log_{10}(I/I_o)$	Detector Height 250 km $\log_{10}(I/I_o)$
100 km	0.0	0.0	0.0
95 km	-0.04	- .08	- .03
90 km	-0.08	- .16	- .06
85 km	-0.12	- .23	- .08
80 km	-0.17	- .29	- .11
Conversion Relative to 200 km	0.0	+0.60	- .35

Stellar Magnitudes = $2.5 \log_{10}(I/I_o)$

Optical Depth = $2.3 \log_{10}(I/I_o)$

Table VI - Calculated Mean Atmospheric Attenuation of Atomic Species (Nighttime - Middle of Sunspot Cycle or Daytime Sunspot Minimum)

$Log_{10}(I/I_o)$ Loss for Vertical Column 95 km to 200 km

Species and Line	Meteor Gas Temperature (°K)					
	1000	3000	5000	7000	10000	13000
H I 1216	1.2	0.56	0.36	0.25	0.15	0.10
N I 1200	2.6	1.00	0.60	0.44	0.27	0.20
O I 1304-6	2.9	1.10	0.64	0.48	0.33	0.25

$Log_{10}(I/I_o)$ Loss for Vertical Column 100 km to 200 km

	Meteor Gas Temperature (°K)					
	1000	3000	5000	7000	10000	13000
H I 1216	1.2	0.50	0.32	0.21	0.14	0.09
N I 1200	2.4	0.90	0.56	0.38	0.25	0.18
O I 1304-6	2.8	1.00	0.60	0.45	0.31	0.24

Notes:

(a) To obtain stellar magnitudes multiply by 2.5

(b) To obtain optical depth multiply by 2.3

(c) Values below 95 km are unknown, loss between 95 km and 100 km is poorly determined, but losses between 100 km and 200 km should be representative.

(d) Solar cycle diurnal and seasonal variations may be as high as ±0.6 in the $\log_{10}(I/I_o)$ value.

C. Far UV Meteor Event Detection Limitations.

In this section, tables which can be used to calculate the frequency of detectable Far UV meteor events are given.

It is assumed that it is possible for a given instrument configuration using the synthetic spectral calculations to be presented later (see Part III) to relate UV luminosity to an apparent magnitude limit (m_{pg}). When such a calibration is available, Tables VII and VIII can be used to find the cumulative rates of meteor detection over a 20 degree field of view from 150 km, 200 km, and 250 km detector heights. These tables contain approximate corrections for the O_2 attenuation and therefore are somewhat pessimistic. Without O_2 corrections the sporadic rates (given in Table VII) would be a factor of two higher, but as can be seen from Table VIII enhancements in rate from the major showers is much more important.

For the near UV, the usual meteor rate calculations [see for example Millman and McKinley (1963); McKinley (1961); Elford (1967); and Lindblad (1967)] upon which Tables VII and VIII are based can be used.

In the evaluation of m_{pg} (limit) for a given instrument configuration, the nature of the background sky is always important. Because of the very low albedo of the earth atmosphere and the moon in the UV (particularly with the observed minimum at 2400 Å where only 10^{-4} of the incident radiation is reflected) moonlight is not expected to be a problem for an earth-looking experiment (see for example Green and Wyatt, 1965b).

A much more severe problem will be nightglow. In Table IX, the expected levels of atmospheric emission for the middle of the solar cycle are presented using the data of Meier (1970) and Fastie (1963). The airglow data can be expected to vary over a factor of two above and below the tabulated values depending on the degree of solar activity. During intense auroral displays a factor of 10^1 to 10^2 may be present.

Table VII - Mean Sporadic
Meteor Detection Rates (per hour)
from Spacecraft
in the Far UV

Limiting m_{pg} of Instrument	Sporadic Meteors per Hour (20° Field of View)		
	200 km	150 km	250 km
0	5×10^{-4}	4×10^{-4}	1.1×10^{-4}
+1	1.3×10^{-2}	1.2×10^{-2}	4×10^{-3}
+2	4×10^{-2}	3.5×10^{-2}	4.4×10^{-2}
+3	0.13	0.10	0.15
+4	0.37	0.23	0.40
+5	0.86	0.44	1.0

Table VIII - Meteor Shower Enhancement Factors
of Detection Rates
in the Far UV

Nighttime Shower Designation	Excitation Class*	Cumulative (Peak Shower Rate) ÷ Cumulative (Sporadic Rate)					
		$m_{pg}=0$	$m_{pg}=1$	$m_{pg}=2$	$m_{pg}=3$	$m_{pg}=4$	$m_{pg}=5$
Quad	Low	0.3	1.5	15	15	19	20
Lyr	Low	6	7	8	8	7	7
η Aqr	High	8	9	10	11	9	9
β Tau	Low	0.0	6×10^{-3}	0.1	1.4	1.6	2
δ Aqu	Low	0.2	0.3	3	3	3	4
Per	High	20	23	25	27	23	22
Ori	High	12	14	15	16	14	13
Leo	High	12	14	15	16	14	13
Gem	Low	0.4	0.8	8	8	9	10
Ursids	Low	0.0	3×10^{-3}	8×10^{-2}	0.7	0.8	1.2

*If geocentric velocity is above 50 km/sec, shower is classified as High Excitation.

Table IX - Strongest Nighttime Airglow Features
Looking Earthward from 200 km

Non-auroral (Meier, 1970)

Identification	λ	I_λ
Ly α	1216 Å	8 kilorayleighs
O I	1304	0.1 kilorayleighs
	1355	0.05 kilorayleighs (est.)

Auroral (Fastie, 1963)

Identification		λ	I_λ
N_2 2nd Pos.	(0-0)	3371.3	0.17 kilorayleighs
	(1-0)	3159.3	0.15 kilorayleighs
O I plus N_2	(1-2)	2976.8	0.15 kilorayleighs
N_2 VK	(0-5)	2603.6	0.04 kilorayleighs
	(0-6)	2760.8	0.04 kilorayleighs
N_2 LBH	1300-1700	1300-1700	$\sim$0.05 kilorayleighs average for each line

Conversions for 20° diameter field of view

Number of photons/sec-cm^2 $\simeq$ 8 x 10^6 x I_λ(kR)

Intensity (ergs/sec-cm^2) $\simeq$ 2 x 10^{-2} x I_λ(kR)/λ(Å)

Possible Solar Cycle and Seasonal Variations of Nightglow

Non-auroral	$\pm$factor of two
Auroral	10^0 to 10^2 enhancements

Text References - Part I

1. Allen, C. W.: Astrophysical Quantities. The Athlone Press, Univ. of London, 1963, p. 78.
2. Cook, G. R.; and Metzger, P. H.: Photoionization and Absorption Cross Sections of O and N in the 600 to 1000 Å Region, J. Chem. Phys., vol. 41, 1964, pp. 321-336.

3. Elford, W. G.: Incidence of Meteors on the Earth Derived from Radio Observations. Meteor Orbits and Dust. Smithsonian Contrib. to Astrophys., vol. 11, 1967, pp. 121-131.

4. Fastie, W. G.: Instrumentation for Far Ultraviolet Rocket Spectrophotometry. J. Quant. Spectrosc. Radiat. Trans., vol. 3, 1963, pp. 507-518.

5. Green, A. E. S.; and Wyatt, P. J.: Atomic and Space Physics, 1965a, p. 410.

6. _____; _____: Atomic and Space Physics, 1965b, p. 510.

7. Herzberg, G.: Spectra of Diatomic Molecules. D. Van Nostrand Co., 1950.

8. Hudson, R. D.: Critical Review of Ultraviolet Photoabsorption Cross-Sections for Molecules of Astrophysical and Aeronomic Interest. NSRDS-NSB 38, 1971.

9. Johnson, F. S.: Satellite Environment Handbook. Stanford Univ. Press, 1961, pp. 18-22.

10. Lindblad, B.-A.: Luminosity Function of Sporadic Meteors and Extrapolation of Influx Rate to Micrometeorite Region. Meteor Orbits and Dust. Smithsonian Contrib. to Astrophys., vol. 11, 1967, pp. 171-180.

11. McKinley, D. W. R.: Meteor Science and Engineering. McGraw-Hill Book Co., 1961, p. 106.

12. Meier, R. R.: Depressions in the Far-Ultraviolet Airglow over the Poles. J. Geophys. Res., vol. 75, 1970, pp. 6218-6232.

13. _____; and Prinz, D. K.: Absorption of the Solar Lyman Alpha Line by Geocoronal Atomic Hydrogen. J. Geophys. Res., vol. 75, 1970, pp. 6969-6979.

14. Millman, P. M.; and McKinley, D. W. R.: Meteors. The Moon, Meteorites, and Comets; The Solar System, vol. IV, The University of Chicago Press (Chicago), 1963.

15. Morton, D. C.: Interstellar Absorption Lines in the Spectrum of Zeta Ophiuchi. Astrophy. J., vol. 197, 1975, pp. 85-115.

16. _____; and Smith, W. H.: A Summary of Transition Probabilities for Atomic Absorption Lines Formed in Low Density Clouds. Astrophy. J. Suppl., vol. 26, 1973, pp. 333-363.

17. Moore, C. E.: A Revised Multiplet Table of Lines of Astrophysical Interest. Contr. Princeton Univ. Obs., no. 20, 1945.

18. _____: Atomic Energy Levels. NBS Circ. 467, sec. 1, 2, 3, 1949, 1952, 1958.

19. _____: An Ultraviolet Multiplet Table. NBS Circ. 488, sec. 1-5, 1950, 1952, 1962.

20. _____: Selected Tables of Atomic Spectra. NSRDS-NBS 3, sec. 1-6, 1965-1972.

21. _____: Ionization Potentials and Ionization Limits Derived from the Analysis of Optical Spectra. NSRDS-NBS 34, 1970.

22. Rosen, B.: Spectroscopic Data Relevant to Diatomic Molecules. Tables de Constants et Donnees Numeriques, vol. 17, Pergamon Press, 1970.

23. Struve, O.; and Elvey, C. T.: The Intensities of Stellar Absorption Lines. Astrophy. J., vol. 79, 1934, pp. 409-440.

Part II. Derivation of a Spectroscopic Temperature Scale for Faint Meteors.

In order to predict the ultraviolet spectrum of a meteor it is necessary to have some understanding of the meteoric excitation mechanism. As shown by Ceplecha (1964, 1967), Harvey (1973a, 1973b) and Millman (1932, 1935), atomic excitation in meteor spectra assumes the characteristics of a Boltzmann distribution in spite of the fact that the situation is collision dominated. Harvey and Ceplecha have used this property to derive effective "radiation" temperatures from meteor spectra as well as attempt to derive meteor elemental abundances.

The spectroscopic classification scheme of Millman (1963) generally indicates that meteor excitation increases with velocity and the Fe I temperatures derived by Harvey (1973) bear this out. Ceplecha (1964, 1973) was the first to recognize that line saturation effects are important particularly for bright meteors. While Ceplecha's model of the meteoric radiating volume is somewhat artificial and his identification of saturation as a *simple* self-absorption effect is suspect, the contention that line saturation of some sort is significant even for a relatively small radiating object such as a meteor is verified by the present study and is in accord with the behavior of certain types of resonance radiation laboratory sources (Mitchell and Zemansky, 1961). The fact that Harvey (1973a) was unable to verify classical self-absorption effects in his spectra indicates the subtlety of the line saturation problem.

The highly successful NASA-LaRC Faint Meteor Spectra Patrol has provided and continues to produce a sufficient quantity of calibrated meteor spectra in brightness and velocity ranges comparable to objects photographed and studied in detail by The Harvard Meteor Patrol project (Jacchia, Verniani, and Briggs, 1967). In addition the problem of deriving abundances and temperatures from meteor spectra shares many common problems with the derivation of abundances in the interstellar medium. As a part of the Copernicus telescope program of Princeton University Observatory groups much of the necessary atomic and molecular physics data is now available for use in meteor physics investigations, particularly with regard to line saturation effects. Given these circumstances, it seemed appropriate as a part of this study of ultraviolet meteor spectra to attempt a re-examination of the meteor temperature problem originally discussed by Harvey (1973a).

The problem of line saturation in absorption was considered in connection with studies of the interstellar medium [Wilson and Merrill, 1937; Strömgren, 1948; Spitzer, 1948] particularly in regard to the Ca II H&K lines and the Na I D lines. However, the principles are applicable to any elementa1 spectral lines which have a similar excitation energy.

A comprehensive theory of meteor line saturation must await a detailed study of LRC faint meteor spectra. However, a brief examination of several *reduced* LRC spectra indicates line saturation to be present for Ca II and Na I in slow meteors (30-40 km/sec) brighter than about $m_{pg} = -2$ and in fast meteors (60-70 km/sec) brighter than about $m_{pg} = 0$. Even N_2, O I, and N I

air radiation in several fast meteors (Harvey, 1976) shows some indications of line saturation.

Direct measurements of the meteor line broadening are not yet available but the fact that even a "low" abundance meteor material such as sodium shows saturation effects in non-resonance as well as resonance lines indicates that meteor kinetic temperatures are never very high.

Because meteor excitation is non-equilibrium, one must be very careful applying traditional curve-of-growth methods in evaluating line-saturation effects. In order to prevent confusion with the classical case of self-absorption in stellar or planetary atmospheres, the term "line-saturation" will be used in the remainder of this report to refer to situations where element lines of equal excitation potential but different statistical weights have comparable intensities. No model of the line transfer problem is proposed at this time. Instead we simply accept the line saturation effects as indicated by the spectra and correct for them in a pure phenomenological way by simply applying approximate corrections to the observational results derived on the assumption of a purely optically-thin plasma (Harvey, 1973b, 1976).

If q_1 and q_2 are the tangents to the appropriate *absorption* curve of growth for the element or molecule it can be shown that the "apparent" temperature T_1 and the collisionally induced radiation temperature T_o are related by the following relationship

$$(q_1E_1 - q_2E_2) \times \frac{5040}{T_o} + (1 - q_1) \log_{10}(gA\lambda^2)_1$$

$$- (1 - q_2) \log(gA\lambda^2)_2 = (E_1 - E_2) \times \frac{5040}{T_1} + \Delta(\log \frac{W}{\lambda})$$

where E_1 and E_2 are the excitation temperatures; $(gA\lambda^2)$ are the respective oscillator strength, wavelength products for these two levels and

$$\Delta(\log \frac{W}{\lambda}) = \log (\frac{W}{\lambda})_{q_2} - \log (\frac{W}{\lambda})_{q_1}$$

with $\log (\frac{W}{\lambda})_{q_2}$ the intercept of the q_2 tangent on the intensity axis and $\log (\frac{W}{\lambda})_{q_1}$ the intercept of q_1 on the intensity axis.

If $q_1 = q_2 = q$ then

$$(1 - q) \log \left(\frac{g_1A_1\lambda_1^2}{g_2A_2\lambda_2^2} \right) - (E_1 - E_2) \times \frac{5040}{T_1} = -(E_1 - E_2) \times \frac{5040q}{T_o}$$

Furthermore, if the line is well-saturated then $q \to 1/2$ is a normal assumption and

$$\frac{1}{2} \log \left(\frac{g_1A_1\lambda_1^2}{g_2A_2\lambda_2^2} \right) - \frac{(E_1 - E_2) \times 5040}{T_1} = - \frac{(E_1 - E_2) \times 5040}{2T_o}$$

With these formulae corrected radiation temperatures may be derived that can be used to determine a scale for faint meteors where line saturation is not a problem.

A. Corrected LaRC Radiation Temperatures.

Using the precepts mentioned above radiation temperatures have been redetermined (by Meisel) from LaRC spectra as a part of this study of meteor ultraviolet emission. The results are as follows.

Meteor Radiation Results

Geminid (m_{pg} = -4, V_∞ = 36 km/sec, near point of maximum light)

Mg I	5000°K	Fe I	2600°K
Ca I	4300°K	Cr I	3600°K

Taurid (m_{pg} = -5, V_∞ = 30 km/sec, one scale height above point of maximum light)

Ca I	5000°K	Mn I	1700°K ?
Fe I	2400°K	Na I	4100°K
Mg I	5000°K		

Perseid (m_{pg} = -9, V_∞ = 60 km/sec, 1.2 scale heights above point of maximum light)

Na I	6000°K	O I	6600°K
Ca I	3400°K	Ni I	2200°K
Mg I	6000°K	Si II	10,000°K
Fe I	2800°K		

Air Radiation Results

Perseid (m_{pg} = 0, V_∞ = 60 km/sec)

N_2 vibrational temperature 9100°K

Also using N_2 $1^+(7,4)$ 6545 Å and N I 6484 Å with $(T_{ext})_{N\ I} = (T_{ext})_{N_2}$ gives $T_{Diss_{N_2}} = 6500°K$

Perseid (m_{pg} = -9, V_∞ = 60 km/sec)

From O I 6156-58, 6454-56 and N I 6482-84 assuming $(T_{ext})_{O\ I} = (T_{ext})_{N\ I}$ we find $T_{Diss_{N_2,O_2}} = 6000°K$

In order to demonstrate the validity of the above values, the abundances derived by Harvey (1973) have been corrected using a mean curve-of-growth and the above temperatures to yield the following abundances:

Elemental Fractions by Number

Element	Taurid	Geminid	Perseid	Average	Carbon. Chon.
Fe I	1.0	1.0	1.0	1.0	1.0
Ni I	1.2×10^{-1}	1.3×10^{-1}	-	1.25×10^{-1}	5×10^{-1}
Ca I	1.2×10^{-4}	1.1×10^{-3}	6×10^{-4}	6×10^{-4}	6×10^{-2}
Mn I	3.3×10^{-4}	4.2×10^{-4}	4.6×10^{-4}	4.0×10^{-4}	6×10^{-3}
Cr I	5.2×10^{-4}	5.2×10^{-4}	5.3×10^{-4}	5.2×10^{-4}	8×10^{-3}
Mg I	0.77	0.92	0.90	0.86	1.0
Si I	2.3	2.1	2.2	2.2	1.0
Na I	3.5×10^{-5}	4.3×10^{-5}	6.9×10^{-5}	5×10^{-5}	3×10^{-2}

These values show good internal agreement in spite of the fact that neither ionization nor oxidation corrections have been applied. Except for Si which is overabundant in the shower meteors, the assumption of a carbonaceous chondrite composition provides realistic upper limits to the meteoroid composition.

B. Other Indications of Meteor Temperature.

Ceplecha (1973) has derived temperatures from a number of fireballs in the m = -10 to -12 range with an average velocity of 30 km/sec, but since the simple line saturation corrections could not be applied with the information available these temperatures cannot be used in this study.

Tagliaferri and Slattery (1969) have produced filter spectra of artificial meteors in free molecular flow. Using the Fe I 2967 Å to Fe I 3720 Å ratio (and assuming in this case no line saturation effects), a value of $T_{ext} \simeq 2700°K$ was derived by Meisel in this UV study for Fe I particles at 30 km/sec.

Air Dissociation

The simplified theory of a dissociating gas flow outlined by Moore (1966) indicates that for equipartition of kinetic energy between dissociated atoms and undissociated molecules there will be two temperatures related by the following expression

$$T_{vib}/T_{kin} = 0.44\ (e^{T_{vib}/T_{kin}} - 1)$$

where T_{vib} is the molecular vibrational temperature and T_{kin} is the average gas kinetic or dissociation temperature. In the case of the LaRC Perseid spectra with $(T_{vib})_{N_2} = 9100°K$ the above expression predicts $T_{kin} = 6200°K$

in excellent accord with the values derived from the N_2/N I and N I/O I ratio. Furthermore we note that the O I radiation temperature is also in excellent accord with the derived T_{kin} and T_{Diss} values. It is therefore concluded that dissociation equilibrium is a valid approximation for meteorically produced air radiation.

Meteoroid Dissociation/Vaporization

Contrary to the assumption used by Harvey (1973a) the corrected temperatures from LaRC spectra do not simultaneously satisfy the equations of dissociation equilibrium using the appropriate properties for elements and oxides calculated from the Handbook of Chemistry and Physics [pps. D45-D73 of 51st (1970-71) edition]. The corrected temperatures do, however, show good correlation with the equations of *element* vaporization (A.I.P. Handbook, 3rd Ed., 1972, p. 4-315). Such a result implies that sputtering is a dominant mechanism of meteoroid gas production for the objects studied. The least dispersion in the observed correlation between T_{ext} (meteoroid element) and the rate of vaporization (meteoroid) [i.e. degree of cooling] occurs when

Object	Velocity	$T_{vaporization}$
Taurid	40 km/sec	5000°K
Geminid	36 km/sec	5500°K
Perseid	60 km/sec	6000°K

It is not clear what meaning to give to such a temperature. However, for the purposes of this study of the meteor ultraviolet we can circumvent the problem of proposing a model of meteor ablation by using the apparent correlation in a simple empirical formula. The excitation temperatures of individual elements in meteors appear to be correlated with the heats of vaporization. A convenient empirical formula from three LRC meteors is

$$T = T_o \, e^{-8.7 \times 10^{-3}(H - H_o)}$$

where T is the element excitation temperature, T_o the same for a reference element, H is heat of vaporization at 25°C in kcal/mole of the particular element and H_o is the same quantity and units for the reference element. An original relationship was derived in terms of thermodynamic properties at 5000°K (derived from Handbook of Chemistry and Physics Table of Thermodynamic Properties) but since most available data on elements is for 25°C, a suitable scaling has been performed.

The nearly universal appearance of Fe I in meteors makes it the most convenient reference element. In Table X we list some of the predicted (T/Fe) values for various meteoroid elements along with their assumed heats of vaporization.

Table X - Heats of Vaporization and Temperature Ratios predicted by empirical formula derived from LRC spectroscopic data (elements used in the determination of the formula are indicated †)

Element	Heat of Vaporization (kcal/mole)*	$(T/T_{Fe})_{spect.}$
Al	78.7	1.2
Be	77.5	1.2
B	136.5	0.7
Ca	42.6	1.6
C	171.3	0.5
Cr†	95.0	1.0
Co	102.4	1.0
H	0.2	2.4
Fe†	99.3	1.0
Mg†	35.0	1.8
Mn†	67.7	1.3
Ni†	102.8	1.0
O	1.6	2.3
N	1.3	2.4
P	42.7	1.6
Si	108.9	0.9
Na†	25.8	1.9
S	66.0	1.3

*At 25°C from the Handbook of Chemistry and Physics, 51st edition (1970-71), p. F-163

In the sputtering process it seems unlikely that a colliding air molecule or atom can distinguish between an elemental fragment and a molecular one. In the absence of a *better* working hypothesis, we therefore assume that molecular fragments will have the same T_{ext} behavior in sputtering as atoms and that the derived empirical formula can be used for molecules if bond energies are used instead of vaporization energies. It remains to be verified that this is indeed the case.

Ionization Temperatures

Corrected ionic and neutral element line ratios in one LaRC spectrum enables a simultaneous solution of the individual Saha equations, assuming T_{ext} (ions) = T_{ext}(Si II) = 10,000°K and T_{ext} (atoms) as tabulated above.

Perseid (m_{pg} = -9, V_∞ = 60 km/sec)
Assuming Ionization Equilibrium for Mg, Ca, Fe, Si, and O gives log N_e = 19.2, $T_{ionization}$ = 5500°K

The similarity of this ionization temperature to those derived from the air radiation is interesting and will be discussed later.

C. A Model of Atomic Excitation for the Case of "Classical" Meteoroids.

An initial attempt at defining a meteor temperature scale was made by Harvey (1973a) assuming optically thin radiation and the validity of the classical meteoroid ablation theory. His results indicate a rather low dependence of $(T_{ext})_{Fe}$ on velocity ($V_\infty^{0.3}$) that is difficult to reconcile with the very high air radiation temperatures obtained in the same objects. A model of meteor excitation is needed first to scale the observed temperatures not taken at maximum light to an equivalent T_{ext} at maximum light and then use those results to find a velocity dependence of $(T_{ext})_{Fe\ I}$ from which the other neutral atom T_{ext} values can be computed.

The "classical" model of ablation (McKinley, 1961) requires that

$$N_m K(T_m + \phi_m T'_m) + N_A K(T_A + \phi_A T'_A) + N_e K T_e = (\tfrac{1}{2} m_\infty V_\infty^2 - \tfrac{1}{2} m V^2)\ [1 - \Lambda - \Lambda'] \quad . \ . \ . \quad (1)$$

N_m = no. of meteor atoms
T_m = meteor atom excitation temp.
T'_m = meteor ion excitation temp.
ϕ_m = fraction of meteor ionization (not necessarily constant)
N_A = number of air atoms (or molecules)
T_A = air excitation temperature
ϕ_A = fractional air ionization (not necessarily constant)

m_∞, V_∞ initial meteoroid mass and velocity

m, V instantaneous meteoroid mass and velocity

N_e, T_e electron density and temperature

Λ = ablation energy fraction

Λ' = ionization energy fraction

If there is no significant coupling of the air and meteoroid radiation fields and ignoring the electron temperature contribution it can be shown at maximum light that the following first approximations hold

$$\text{(a)} \quad \left(T_A\right)_{mL} \simeq \text{constant with height and angle of incidence} \quad \ldots (2)$$

$$\text{(b)} \quad \left(T_A\right)_{mL} \propto V^2 (1 - \Lambda - \Lambda') \quad \ldots (3)$$

$$\text{(c)} \quad \left(T_m\right)_{mL} \propto A V^3 \rho_a' (m_\infty)^{-1/3} (\mu_m/\mu_A) [1 - \Lambda - \Lambda'] \cos\theta \quad \ldots (4)$$

where A = aerodynamic shape factor, ρ_a' = atmospheric density at maximum light, m_∞ = initial mass, ξ_m = the mean molecular weight of the meteoroid, μ_A = mean molecular weight of air at maximum light, and θ is the angle of incidence into the atmosphere.

For meteoroids which show "classical" behavior we assume $A (\mu_m/\mu_A)[1 - \Lambda - \Lambda']$ is constant and $\rho_a' \propto m_\infty^{1/3}/V_\infty^2$. Consequently

$$\left(T_m\right)_{mL\ \text{classical}} \propto V_\infty \left(\frac{\langle \rho_m \rangle}{\rho_m}\right)^{2/3} \quad \ldots (5)$$

where $\langle \rho_m \rangle$ is the average meteoroid density and ρ_m is the density for a particular meteor. In the "classical" meteoroid model, a mass law of the form

$$m = m_\infty \left(1 - \frac{\rho_a}{3\rho_a'}\right)^3 \quad \ldots (6)$$

where ρ_a' is the atmospheric density at maximum light and ρ_a is the atmospheric density at the height where the mass is m.

Except for the Virginids, Geminids, Orionids and Draconids, the Super-Schmidt results (Jacchia, Verniani, and Briggs, 1967) indicate that there is a correlation of ρ_m with V such that

$$\frac{\langle \rho_m \rangle}{\rho_m} \propto V_\infty^{-0.75} \quad \ldots (7)$$

which predicts that for classical non-fragmenting meteoroids from showers one should find

$$\left(T_m\right)_{mL} \propto V_\infty^{0.5} \quad \ldots (8)$$

The $V_\infty^{0.3}$ correlation used by Harvey seems in agreement with this relationship. It should be noted that in the classical meteoroid case neither the air radiation temperature nor the meteoroid temperatures are a function of mass. It is also of interest to note that the air radiation temperature should have a V_∞^2 variation and be virtually height and inclination independent behavior.

$$T(h) = T_o(h')_{mL} \frac{[1 + \frac{1}{3}e^{\frac{-(h-h')}{H}} - \frac{1}{27}e^{\frac{-2(h-h')}{H}}]}{[1 - \frac{1}{3}e^{\frac{-(h-h')}{H}} + \frac{1}{27}e^{\frac{-2(h-h')}{H}}]} \quad \ldots (9)$$

where H is the assumed atmospheric scale height.

In the "classical" meteoroid theory it is *tacitly* assumed that the heat of ablation is constant. This can hardly be the case, particularly since the LaRC spectra indicate a correlation between excitation temperature and heat of vaporization. The different heat of ablation for each element will make the maximum light for each element occur at slightly different heights in the atmosphere such that if h' is taken as the height of maximum Fe I radiation at $\rho_a = \rho_a'$ then an element with heat of vaporization ζ will reach maximum light at a height with density $\rho_a = \rho_a''$. In the "classical" theory the rates of mass loss must all be equal at maximum light so that

$$\frac{\zeta}{\zeta_o} = \frac{\rho_a''}{\rho_a'} = e^{\frac{-(h''-h')}{H}} \quad \ldots (10)$$

where $_o$ is the heat of vaporization of iron. This approximation leads to

$$T(h,\zeta) = T(h,\zeta_o) \frac{[1 - \frac{1}{3}\frac{\zeta}{\zeta_o} + \frac{1}{27}\frac{\zeta}{\zeta_o^2}]}{[1 + \frac{1}{3}\frac{\zeta}{\zeta_o} - \frac{1}{27}\frac{\zeta^2}{\zeta_o^2}]} \quad \ldots (11)$$

as a prediction of the heat of vaporization dependence of temperature. While the height dependence of the temperature (a) depends critically on the chosen H value, the heat of vaproization dependence does not.

In Table XI the height-temperature dependence of a classical meteoroid is presented assuming that H=6.

If, as is the case for photoelectric intensities such as those derived from the Tagliaferri and Slattery (1969) results, one integrates the spectral intensities over the entire meteor trail, the "apparent-integrated" temperature will be the mass average. Thus

$$\langle T_m \rangle_{obs} = 0.71 \times T_m(h')$$

In addition there is a cosine factor which takes into account the inclination of the meteor path to the atmosphere.

Table XI -
Height-Temperature Dependence Predicted by
Classical Meteoroid Theory

Classical Mass Fraction m/m_∞	$\frac{H=6\text{ km}}{(h-h')}{H}$	$(h-h')$	Meteoroid $\frac{T_m(h)^*}{T_{m_o}(h')}$	Air $\frac{T_A(h)^*}{T_A(h')}$	Parameters for H=6 km: $\Delta t \cos x$ sec 40 km/sec	$\Delta t \cos x$ sec 50 km/sec	$\Delta t \cos x$ sec 60 km/sec	$\Delta t \cos x$ sec 70 km/sec
8×10^{-4}	-1.0	-6 km	2.2	.82	0.15	+0.12	+0.10	+0.09
4×10^{-2}	-0.67	-4	1.6	.96	0.10	+0.08	+0.06	+0.06
0.15	-0.33	-2	1.2	.98	0.05	+0.04	+0.03	+0.03
0.30	0.0	0	1.00	1.00	0.0	0.0	0.0	0.0
0.44	0.33	+2	0.87	1.02	-0.05	-0.04	-0.03	-0.03
0.57	0.67	+4	0.78	1.03	-0.10	-0.08	-0.06	-0.06
0.68	1.0	+6	0.71	1.03	-0.15	-0.12	-0.1	-0.09
0.75	1.33	+8	0.66	1.03	-0.20	-0.16	-0.13	-0.12
0.823	1.67	+10	0.63	1.04	-0.25	-0.20	-0.17	-0.15
0.871	2.00	+12	0.61	1.04	-0.30	-0.22	-0.20	-0.18

*Includes an approximate correction for deceleration

$$\langle T_m \rangle_{obs} = 0.71\ T_m(h',0)\ \cos\theta_{obs}$$

Thus $$T_m(h',0) \simeq 1.41\ \frac{T_{m\ obs}}{\cos\theta_{obs}}$$

where $\langle T_m \rangle_{obs}$ is the temperature determined by integration over the entire meteor, θ is the angle of incidence of the meteor. A similar expression can be obtained for the air radiation but without the cos θ factor (correct to first order).

$$\langle T_A \rangle_{obs} = 1.02 \times T_A(h',0)$$

and $$T_A(h',0) \simeq 0.98\ \langle T_A \rangle_{obs}$$

With a height-temperature dependence relationship, the iron temperature results can be scaled to obtain (T_{mL}).

For four showers (Draconids, Virginids, Geminids, Orionids) the departures from the $m = m_\infty(1 - \rho_a/3\rho_a')^3$ law are so severe it is necessary to provide additional corrections.

Table XII - Adjustments to the Classical Theory

Shower	$\left(\frac{h-h'}{H}\right)$ Factor	$\left(T_{mL}\right)_{Fe}$ Factor
Draconids	0.9	1.52
Virginids	1.2	0.86
Geminids	1.3	0.62
Orionids	1.3	1.28

In Table XIII we present a comparison of the temperature ratios predicted by the spectroscopic formula (derived earlier from LaRC spectra) and those predicted by expression (11). The agreement between the ablation theory and the spectroscopic formula seems to be quite acceptable.

In Table XIV the corrected zenithal temperatures derived from LaRC spectra where (h-h')/H could be found by direct scaling from the light curve are presented and compared with the Fe simulated meteors produced by Tagliaferri and Slattery (1969). The velocity dependence of these $(T_{Fe})_{mL}$ results, unfortunately, does not agree with the predicted $V_\infty^{0.5}$ variation. However, since the $V_\infty^{0.5}$ variation should represent a useful lower bound to meteor excitation, the results predicted by the "classical" meteoroid theory are given in the table using the Taurid result for the Fe temperatures and Perseid results for air temperatures.

Table XIII
Corrections for Vaporization Effect

Element	ζ/ζ_{Fe}*	Ablation Model $\frac{T}{T_{Fe}}$	Spectroscopic Data Fitting $\frac{T}{T_{Fe}}$	Remarks
Al	0.80	1.2	1.2	
Be	0.78	1.2	1.2	
B	1.36	0.9	0.7	
Ca	0.43	1.5	1.6	Also ionic
C	1.73	0.7	0.5	
Cr	0.96	1.1	1.0**	
Co	1.03	1.0	1.0	
H	0.002	2.0	2.9	Hα observed
Fe	1.00	1.0	1.0**	Sometimes ionic
Mg	0.35	1.6	1.8**	Also ionic
Mn	0.69	1.3	1.32**	Sometimes ionic
Ni	1.04	1.0	1.0**	
O	0.02	1.9	2.3	Observed in air radiation
N	0.01	1.9	2.3	Observed in air radiation
P	0.43	1.5	1.6	
Si	1.10	1.0	0.9	Also ionic
Na	0.26	1.6	1.9**	
S	0.67	1.3	1.3	
Cu	0.82	1.2	1.2	
Zn	0.31	1.6	1.8	
H_2O	0.11	1.8	2.2	
CO_2	0.06	1.9	2.2	
$H_2O \rightarrow H + OH$	1.20	0.9	0.8	
$CO_2 \rightarrow CO + O$	1.28	0.9	0.8	
$OH \rightarrow H + O$	1.03	1.0	1.0	
$CO \rightarrow C + O$	2.58	0.5	0.2	
SiO_2	0.03	1.9	2.3	
$SiO_2 \rightarrow SiO + O$	0.30	1.6	1.8	
$SiO \rightarrow Si + O$	1.90	0.7	0.5	
SO_2	0.06	1.9	2.2	
$SO_2 \rightarrow SO + O$	1.26	0.9	0.8	
$SO \rightarrow S + O$	1.25	0.9	0.8	
$FeS \rightarrow Fe + S$	0.79	1.2	1.2	

*Calculated from Heats of Vaporization and bond energies (ζ_{Fe} = 99 kilocalories/mole)

**Elements used in the empirical fitting from photographic spectral analysis results

Table XIV - Corrected Zenithal Temperatures for Iron

Meteor	$\langle T_{Fe} \rangle_{obs}$	cos θ	Zenith T_{Fe} °K	Correction to Maximum Light	$(T_{Fe})_{mL}$ (°K)	V_∞
Taurid	2400°K	0.93	2600	1.4	3600	30 km/sec
Geminid	2600°K	0.95	2700	(1.6)*	(4300)*	36
Perseid	2800°K	0.62	4500	1.5	6800	60
Fe Artificial	2700°K	1.00	2700	1.4	3800	27

*Does not follow the classical formula for m/m_∞.

Table XV -
Predicted Iron and Air Temperatures
for Non-Fragmenting Meteoroids (Classical Theory)

Shower	Maximum-Light Temperatures (Vertical Incidence)		$\langle \cos \theta \rangle$ +	Maximum-Light Temperatures (Average Incidence)	
	Iron (°K)	Air (°K)		Iron (°K)	Air (°K)
Quadrantid	4500	4500	0.6	2700	4500
Virginid	(3200)*	2400	0.7	(2200)*	2400
Lyrid	4800	5900	0.9	4300	5900
η Aqr	5600	10800	0.4	2200	10800
δ Aqr	4400	4500	0.6	2600	4500
α Cap	3400	1700	0.7	2400	1700
i Aqr	4000	2900	0.5	2000	2900
Perseid	5300	8800	0.7	3700	8800
κ Cyg	3300	1300	0.5	1600	1300
Draconid	(4600)*	980	0.7	(3200)*	980
Orionid	(7200)*	10800	0.6	(4300)*	10800
Taurid	3100	2200	0.8	2500	2200
Leonid	5800	12700	0.9	5200	12700
Geminid	(2500)*	3100	0.9	(2200)*	3100
Sporadic					
40 km/sec	4300	4000	0.66	2800	4000
60 km/sec	5300	9000	0.66	3500	9000

*Values corrected for abnormal ablation using data from Jacchia, Verniani, and Briggs (1967)

+Taken from Super-Schmidt meteor data by Jacchia, Verniani, and Briggs (1967) for northern hemisphere stations.

$$T_{Fe}(°K)_{mL,\ Zenith} = 680\ V_\infty^{1/2} \quad \ldots (12)$$

$$T_{Air\ mL,\ Zenith} = 2.5\ V_\infty^2 \quad \ldots (13)$$

D. Atomic Excitation of a Fragmenting Meteoroid.

Meteor fragmentation seems to be well established both for photographic and radio studies of meteors (Jacchia, 1955; Hawkins and Southworth, 1958; Jones and Kaiser, 1966; Lebedivec and Portnyagin, 1968; Verniani, 1969, 1973; and Jones and Hawkes, 1975) to explain the shortness of meteor trails compared to the classical light curves.

The radio results of Verniani (1973) and the low-light-level television results of Jones and Hawkes (1975) show that for faint objects, the classical theory is unsuitable for explaining meteor light curves. However, one can scale the classical meteoroid results first to the photographic results and then to television meteors by simply adopting a fragmentation scale height H_f and using it instead of the usual scale height H. Such a procedure was first used by Cook, Jacchia, and McCrosky (1963). The available TV and photographic light curves appear to satisfy an empirical relationship

$$H_f = 3.5 - 0.2\ M_{pg} \quad \ldots (14)$$

Since M_{pg} is also correlated with the atmospheric height (and hence the scale height) at maximum light we propose that

$$H_f = 4.7 - 0.2\ M_{pg} - 0.8 \log V_\infty(\text{km/sec}) - 0.1 \cos \theta \quad \ldots (15)$$

as a reasonable empirical representation for H_f.

In order to make the fragmentation tractable the following assumptions are made.

(a) Progressive fragmentation can be replaced by an equivalent single disintegration.

(b) Enhancement of the observed meteor light output above that predicted by classical theory is due entirely to an increase in the effective exposed area of the meteoroid with each fragment behaving classically with properties identical to the original.

(c) Loss of trapped air is complete at fragmentation.

Under such conditions the temperature of a fragmented meteoroid $T_f(h)$ is related to the classical value by

$$Tm(h)_f = Tm(h)\left(\frac{V(h)_f}{V(h)}\right)^3 \frac{(\rho a')_f}{(\rho_{a'})} \frac{m(h)}{m(h)_f} \left[\frac{\Sigma\left(\frac{mf}{\rho_{mf}}\right)^{2/3}}{\left(\frac{m}{\rho_m}\right)^{2/3}_h}\right] \quad \ldots (16)$$

Here the subscript f indicates values of V, ρ'_a, m, and ρ_m referring to the fragments.

First note that

$$\frac{(\rho'_a)_f}{(\rho'_a)} = e^{\frac{-(h'_o-h')}{H}} \quad \ldots (17)$$

where h'_o is the observed height of maximum light and h' is the height of maximum light given by McKinley's (1961) formula

$$h' = 23 + 44 \log_{10} V_\infty(\text{km/sec}) + 1.8 (m_{pg})_{max}$$

and H is the fragmentation scale height.

Under assumption (b) from McCrosky and Sobermann (1963)

$$\frac{\Sigma_i\left(\frac{m_f}{\rho_{mf}}\right)^{2/3}}{\left(\frac{m}{\rho_m}\right)^{2/3}} = \frac{V^6}{V_f^6}\left[\frac{I_f}{I_o}\right] \quad \ldots (18)$$

where I_f is the light output with fragementation and I_o is the light output of an equivalent unfragmented meteoroid. Thus

$$Tm(h)_f = Tm(h)\left(\frac{V}{V_f}\right)^3 \frac{m(h)}{m(h)_f}\left[\frac{I_f}{I_o}\right] e^{\frac{-h'_o-h'}{H}} \quad \ldots (19)$$

is obtained as an intermediate result. Since deceleration will be more important for fragmentation the usual $V \to V_\infty$ approximation will not be made. As noted by Verniani (1961) and Evans (1967) the meteor mass ratio can be approximated by

$$\frac{m(h)}{m(h)_f} = e^{\frac{-(V_f^2 - V^2)}{4\xi}} \quad \ldots (20)$$

where ξ is the deceleration constant which averages 16 km^2/sec^2. Further substitution and the approximation that

$$\frac{m(h)}{m(h)_f} \simeq \frac{\left(1 - \frac{1}{3} e^{\frac{-(h-h')}{H}}\right)^3}{\left(1 - \frac{1}{3} e^{\frac{-(h-h'_o)}{H}}\right)^3} \quad \ldots (21)$$

gives another intermediate result

$$Tm(h)_f = Tm(h) \left[1 - \frac{62}{(V_\infty^2-75)} \log_e \left(\frac{m(h)}{m(h)_f}\right)\right]^{-3/2} \frac{m(h)}{m(h)_f} e^{\frac{-(h_o'-h')}{H}} \left[\frac{I_f(h)}{I_o(h)}\right] \quad . . . (22$$

If the fragments are identical to each other and to their parent bodies except for mass, the definition of photometric mass requires that at maximum light

$$\left[\frac{I_f}{I_o}\right]_{mL} = \frac{V_\infty^3}{V_{\infty_o}} \frac{(m_\infty)^{1+\chi}}{(m_\infty)_o^{1+\chi_o}} \frac{e^{0.92\, m_{pg}}}{e^{0.92 (m_{pg})_o}} \quad . . . (23)$$

where χ is the progressive fragmentation index defined by Jacchia, Verniani, and Briggs (1967) and the subzero indicates the quantities for a suitable low fragmentation group taken here to be the N. Taurids. At maximum light therefore

$$\left(Tm(h_o')\right)_{f_{mL}} = Tm(h_o') \, e^{\frac{-(h_o'-h')}{H}} \left[1 - \frac{62}{(V_\infty^2-75)} \log_e \frac{m}{m_f}_{mL}\right] \left(\frac{m}{m_f}\right)_{mL} \left[\frac{V_\infty^3}{(V_\infty)^3_{Tau}} \frac{m_\infty^{1+\chi}}{m_{\infty_{Tau}}^{1+\chi_{Tau}}}\right.$$

$$\left. \times \, e^{0.92\,(m_{pg}-m_{pg\ Tau})}\right] \quad . . . (24)$$

$$\text{with } \left(\frac{m}{m_f}\right)_{mL} = 3.38 \left(1 - e^{-(h_o'-h')}\right)^3 \quad . . . (25)$$

As a check on the suitability of expressions (24) and (25), the photographic data presented by Jacchia, Verniani, and Briggs (1967) have been used to calculate $T_{mL}/(T_{mL})_{Tau}$ for 17 meteor showers and the average sporadic meteor. The results shown in Figure 1 and listed in Table XVI show the calculations for the N. Taurids, Geminids, Perseids, Orionids, and Leonids (Group I) to be in good agreement with the available observational values listed in Table XIV. The best fit of the observed temperature values is

$$(T_{Fe})_{Zenith}\ (°K) = 231\ V_\infty^{0.81}\ (km/sec) \quad . . . (26)$$

which is intermediate between the $V_\infty^{0.5}$ variation predicted by "classical" theory and the $V_\infty^{+0.96}$ slope of the results calculated assuming complete fragmentation occurs. Although the calculated results for other showers appear anomalously low, one can see an approximate V_∞^{+1} trend among the S. Taurids, Virginids, Lyrids, and α Capricornids (Group II) and also for the κ Cygnids, i Aquarids, Quadrantids, σ Hydrids, and η Aquarids (Group III).

In the next section, an explanation why the fragmentation calculations introduce systematic effects for Groups II and III is given. Certainly the

classification scheme of Millman (1963) shows that the Lyrids, Quadrantids, and S. Aquarids have excitations comparable to the Taurids (with no distinction between northern and southern components). Just *exactly* how much systematic adjustment is necessary to bring the calculations for Group II and Group III in accord with observation must be determined when high resolution Group II and Group III spectra become available.

In order to obtain a "universal" temperature curve, the following *ad hoc* (for the moment) systematic corrections to the fragmentation calculations are required to bring the results into average agreement:

Group II $\quad \Delta\log T_{Fe}/(T_{Fe})_{Tau} = + 0.4$

Group III $\quad \Delta\log T_{Fe}/(T_{Fe})_{Tau} = + 0.9$

Since the air radiation temperature is virtually unaffected by the fragmentation a *provisional* temperature scale suitable for calculation of the ultraviolet meteor spectrum is defined by the previously quoted expressions

$$(T_{Fe})_{mL,\ Zenith} = 231\ V_\infty^{0.8} \text{ (km/sec)} \qquad \ldots (26a)$$

and $$(T_A)_{mL,\ Zenith} = 2.5\ V_\infty^2 \text{ (km/sec)} \qquad \ldots (27)$$

Finally we note that the temperature-height relationship of a fragmenting meteor will simply be that using the fragmentation scale-height H_f instead of the atmospheric scale height. Thus all one has to do is find H_f and then read the appropriate (T/T_{mL}) ratio opposite the $(h-h')/H_f$ in Table XI. Since $H_f < H$, the temperature rise of a fragmenting meteor will always be faster than for a classical meteoroid. Because T(h) is inexorably bound to I(h) even with fragmentation, when I(h) is roughly constant T(h) will be also.

E. Comments on the Computed Temperature Ratio Discrepancy and the Suitability of the Adopted Temperature Scale.

The masses tabulated for various showers by Jacchia, Verniani, and Briggs (1967) and used in the temperature ratio (fragmentation) calculations were all scaled using a common value of the luminous efficiency [Verniani, 1964; $\tau_p = 10^{-19}\ V_\infty(\text{cm/sec})$]. Although differences in meteoroid properties could perhaps alter $A(1 - \Lambda - \Lambda')$ and therefore change $T_{Fe}/(T_{Fe})_{Tau}$ [For example, it is almost certain that for the Draconids that $A > 1$ and $\Lambda \to 0$ is responsible for part of their higher than "normal" calculated $T_{Fe}/(T_{Fe})_{Tau}$.], such a possibility for a factor of ten hardly seems possible. Considering the difficulties involved in scaling the various artificial meteor [Ayers, McCrosky, and Shao (1970)] and laboratory determinations (Friichtennicht and Becker, 1973: Savage and Boitnott, 1973 represent two recent discussions),

it seems natural to examine the $T_{Fe}/(T_{Fe})_{Tau}$ discrepancy as an indication of a possible luminous efficiency variation between Groups I, II, and III. The *ad hoc* temperature adjustments applied in the previous section require that for

$$[(T_{Fe})/(T_{Fe})_{Tau}]_{obs} = [(T_{Fe})/(T_{Fe})_{Tau}]_{cal}$$

it is necessary that

$$\left.\begin{aligned} \tau_{Group\ II} &= 0.4\ \tau_{Group\ I} \\ \tau_{Draconid} &= 3.1\ \tau_{Group\ I} \\ \tau_{Group\ III} &= 0.13\ \tau_{Group\ I} \\ \tau_{Sporadic} &= 1.8\ \tau_{Group\ I} \end{aligned}\right\} \quad \ldots (28)$$

where τ is the luminous efficiency at a given velocity.

Using the Fe artificial meteor luminous efficiency curves of Friichtenicht and Becker (1973) to scale the low-velocity viscous flow results of Ayers, McCrosky, and Shao (1970), Cook, Jacchia, and McCrosky (1963), and McCrosky and Sobermann (1963) on both natural and artificial meteors to the higher velocity free-molecular regime, indicates that the assumed Verniani (1964) luminous efficiency corresponds to an approximate iron abundance of about 1/3 by number. Considering the assumptions required to scale the low velocity results, the fact that the revised abundances given earlier for the Group I objects (Taurid, Geminid, and Perseid) have an iron fraction of 1/4 is considered good enough agreement to postulate that at least some, if not all, of the $(T_{Fe})/(T_{Fe})_{Tau}$ discrepancy is due to an iron abundance difference between Groups I, II, and III. Such a view predicts that Group II will be relatively iron poor and most sporadic meteors will be relatively iron rich.

Certainly the abundance derived from one sporadic meteor (Harvey, 1973a, 1973b) does seem to be iron-rich and the Fe simulated meteor position is slightly above the mean temperature-velocity relation of Group I.

It is interesting to note that if one takes ratios of the experimentally determined luminous efficiencies at 40 km/sec for Na, Fe, Ca, and Mg derived by Savage and Boitnott (1973) with that of Fe corresponding to Group I objects, an unmistakable pattern emerges.

Meteoroid Group in Figure 1	Dominant Element in Light Curve	Experimental(*) τ/τ_{Fe}	$\tau/\tau_{Group\ I}$ (†)
Draconids	Na	3.3	3.0
Group I	Fe	1.0	1.0
Group II	Ca	0.4	0.4
Group III	Mg	0.12	0.13

*Savage and Boitnott (1973) †This present investigation

The agreement can hardly be coincidental, but the mechanism is not understood. However for the present we conclude that the photometric masses derived from the Super-Schmidt results (Jacchia, Verniani, and Briggs, 1967) are systematically affected by the activation dominance of particular elements in the photographic light curves. Harvey (1974) has shown that such strong differentiation exists in high velocity meteoroids. If one accepts the elemental correlation between the uncorrected temperature ratio groups as real, the orbital identification of both Taurid showers with P/Comet Encke and the Orionids and η Aquarids with P/Comet Halley indicates a process of *progressive* differentiation is required.

If one makes the appropriate corrections to the photometric masses, one obtains a single $T_{Fe}/(T_{Fe})_{Tau}$ - temperature relationship that even the Draconids satisfy (Figure 2).

The adopted *provisional* temperature scale with $V_\infty^{0.8}$ therefore is a suitable compromise between the predicted $V_\infty^{0.5}$ temperature variation for non-fragmenting meteoroids and the predicted V_∞^{+1} for completely fragmenting meteoroids.

Table XVII gives the predicted Fe temperatures for completely fragmenting meteors based on a V_∞^{+1} variation. It should be noted that no special corrections are required for the Virginids, Geminids, Orionids, or Draconids as was the case for the "classical" non-fragmenting model.

Furthermore, the use of the fragmentation scale height H_f to scale the temperature-height behavior also permits the heat-of-vaporization - temperature scaling to be used without modification for the case of completely fragmented meteoroids.

Table XVI - Calculated Temperature Ratio
Relative to Taurids for
Completely Fragmented Meteoroids

Shower	V_∞ (km/sec)	Observed Height of Maximum Light	$\frac{T_{mL}}{(T_{mL})_{Tau}}$	Luminous Efficiency Normalizing Factor (+)	$\frac{(T_{mL})_{Norm}}{(T_{mL})_{Tau}}$	Group/ Element Class
Quadrantids	43	96 km	0.12	7.7	0.92	III, Mg
Virginids	31	84	0.49	2.5	1.2	II, Ca
Lyrids	49	97	0.65	2.5	1.6	II, Ca
η Aqr	67	102	0.45	7.7	3.5	III, Mg
δ Aqr	42	93	0.18	7.7	1.4	III, Mg
α Cap	26	90	0.30	2.5	0.75	II, Ca
S. i Aqr	34	90	0.13	7.7	1.0	III, Mg
N. i Aqr	36	90	0.19	7.7	1.5	III, Mg
Perseids	60	99	2.1	1.0	2.1	I, Fe
κ Cyg	23	89	0.16	7.7	1.2	III, Mg
Draconids	20	97	2.3	0.3	0.69	I?, Na
Orionids	68	106	2.6	1.0	2.6	I, Fe
S. Taurids	30	88	0.48	2.5	1.2	II, Ca
N. Taurids	31	83	1.0	1.0	1.0	I, Fe
Leonids	72	89	3.8	1.0	3.8	I, Fe
σ Hydrids	59	93	0.26	7.7	2.0	III, Ca
Geminids	36	86	1.5	1.0	1.5	I, Fe
Mean Shower	39	92	1.0	1.0	1.0	I?, Fe
Mean Sporadic	34	89	1.9	1.0	1.9	I?, Fe
Notes	*	*	(a) (+)	(++)	(b) (++)	(+) (++)

* From Jacchia, Verniani, and Briggs (1967)
(+) See text, Section D for details
(++) See text, Section E for details

(a) Plotted in Figure 1
(b) Plotted in Figure 2

Table XVII -
Predicted Fe Temperatures--Complete Meteoroid Fragmentation

Shower	Maximum-Light Temperatures (Vertical Incidence)		$\langle \cos \theta \rangle$+	Maximum-Light Temperatures (Average Incidence)	
	Iron (°K)	Air (°K)		Iron (°K)	Air (°K)
Quadrantid	5200	4500	0.6	3100	4500
Virginid	3700	2400	0.7	2600	2400
Lyrid	5900	5900	0.9	5300	5900
η Aqr	8000	10800	0.4	3200	10800
δ Aqr	5100	4500	0.6	3100	4500
α Cap	3100	1700	0.7	2270	1700
i Aqr	4200	2900	0.5	2100	2900
Perseid	7200	8800	0.7	5000	8800
κ Cyg	2800	1300	0.5	1400	1300
Draconid	2400	980	0.7	1700	980
Orionid	8200	10800	0.6	4100	10800
Taurid	3600	2200	0.8	2900	2200
Leonid	8600	12700	0.9	7700	12700
Geminid	4300	3100	0.9	3900	3100
Sporadic					
40 km/sec	4700	4000	0.66	3100	4000
60 km/sec	7200	9000	0.66	4800	9000

$$(T_{Fe})_{Zenith} = 120\ V_{\infty}$$

+Taken from Super-Schmidt meteor data by Jacchia, Verniani, and Briggs (1967)

F. Molecular Radiation

In view of the correlation of excitation temperature with *elemental* heat of vaporization, it seems that the original molecular state of the meteoroid is not very important in determining the state of excitation of atomic meteoric species.

Although several reported unidentified spectral features (Harvey, 1973a) may eventually be shown to be molecular and of meteoric origin, a recent personal examination of LaRC faint meteor spectra failed to show any strong positive evidence for well developed molecular band structure of possible *meteoroid* origin even in low velocity objects. While the sputtering mechanism itself is not clear at this point, its thermodynamic consequences appear to severely limit molecular survival (or formation) to those combinations with positive heats of formation or those whose chemical bond energies are less than the respective *elemental* heats of formation. Such compounds are for the most part very unusual and with the exception of perhaps H_2O are not expected to be found in meteoric spectra. For future reference however, we list the compounds which are most likely to survive the sputtering process leading to the heat-of-formation and excitation temperature correlation.

List of Substances Thought Capable of Surviving Sputtering in Faint Meteoroids

AlN	Fe_2N
Al_4C_3	$Fe_{0.95}O$ (wüstite)
CaC_2	FeS_2 (Pyrites)
CaH(*)	FeSi
CaN_6	MgH(*)
$CaSi_2$	MgS?
C_2	Mn_3C
CO	MnO(*)
Cr_2N	Ni_3C
COH	NO (*)
CO_3C(*)	NO_2 (*)
CuH(*)	N_2O_4(*)
CuO(*)	N_2O (*)
$Cu(OH)_2$(*)	O_3 (*)
H_2O?	SiH_4
Fe_3C(*)	SiC, SiN, Si_2
	H_2S

(*) indicates a strongly positive heat of formation

Of these only FeO has ever been identified (Harvey, 1973b). In shock tube experiments using a variety of materials, molecular features were distinctly absent in a meteorite spectrum although bands of some sort were nearly always present in other powdered samples (Nicholls, Parkinson, and Reeves, 1963).

A list such as that above gives no idea of what molecular species might be expected to show up while dissociation is taking place. Until firm obser-

vations of meteoroid molecular species become available from which the necessary production and excitation relationships can be derived, it seems best to assume that molecular bond energies are analogous to elemental heat of vaporization (or formation) in the excitation temperature relations derived earlier.

Predicting the survival of even diatomic meteoric species in dissociating air is in its simplest approximation a very complicated problem (Green and Wyatt, 1965; Moore, 1966 for example) and it is obvious that much remains to be explored in the chemistry of the meteor environment. We can, however, state based on the earlier air dissociation results, that for $V_\infty > 35$ km/sec one is dealing with nearly complete O_2 dissociation of air and so the problem of absorption by hot O_2 and NO molecules can be safely ignored. In slow meteors, not only is it likely that hot O_2 and NO in the meteor plasma may be a problem, but the low excitation temperatures available and the greater atmospheric penetration serve to limit consideration of far-UV emission to meteors with velocities in excess of 40 km/sec.

G. Ionization and Ionic Excitation

The problem of meteor ionization from a spectroscopic viewpoint has been considered in some detail. The discussions by Cook (1955), Rajchl (1963, 1964), and Baker (1959) consider a direct charge exchange process while Hoffman (1971) following the suggestion by Hoffman and Longmire (1968) favors a two-step charge exchange which enhances certain ionic lines preferentially as described by Harvey (1971). Mitchell and Zemansky (1961) have discussed collisional effects on resonance lines in some detail. Both quenching of lines by a foreign gas and enhancement of at least two ionic species (copper and aluminum) have been observed in laboratory experiments (Mitchell and Zemansky, 1961) and are most easily ascribed to collision processes. One must be careful, however, in attempting to scale such relatively "low" temperature results to higher temperature dissociating air mixtures where unobserved negative ion formation may occur (Green and Wyatt, 1965; especially pps. 578-601 and Chapter 3; Whitten and Poppoff, 1971) in addition to the usual positive ion and molecule formation. Since none of these theoretical treatments is really suitable for predicting the UV spectra of ionic species in meteors, a semi-empirical approach will be adopted once again in an attempt to circumvent the requirements of a detailed ionization model.

In the ultraviolet meteor problem for reasons previously mentioned, only objects with $V > 40$ km/sec need to be considered. Furthermore since at maximum light a large amount of the O_2 is dissociated for $V > 35$ km/sec, it is assumed that only N_2^+ collisions are important in ionization. In the direct collision mode ($N_2^+ + Y \rightarrow N_2 + Y^+$) the following reactions are possible.

*H I → H I	†C I → C II
†O I → O II	*Na I → Na II
†N I → N II	Al I → Al II
Mg I → Mg II	*Mg II → Mg III
Ca I → Ca II	*Ca II → Ca III
Si I → Si II	*Ti II → Ti III
*S I → S II	*Mn II → Mn III
Fe I → Fe II	V I → V II
Ti I → Ti II	*Mn I → Mn II
*Cr I → Cr II	

*Indicates a depletion reaction, product not observable
†Indicates ionization energy is available but an inelastic collision is required to leave ion in an observable state

The two-step ionization model (Hoffman, 1971) is much more restrictive since the lowest energy mode (N_2^+ in ground state) requires

$$E_{\text{ionization of atom}} + E_{\text{excitation of atom}} = E_{\text{recombination of } N_2^+} - E_{\text{excitation of } N_2} \pm \Delta E'$$

where ΔE is a small energy difference usually supplied by thermal energy if needed. Only three features easily satisfy the above condition.

Ca II	3933, 3968 Å
Mg II	4481 Å (requires some thermal energy)
Si II	6347 Å (requires some thermal energy)

In addition Fe II 5316 Å, Fe II 4233 Å, and Si II 4130 Å could satisfy the above energy criterion if a (non-thermal?) source energy of up to +1.5 keV were available, but Fe II 4233 and Si II 4130 do not easily satisfy spin conservation requirements in the collision with N_2^+.

We do not intend to discuss the relative merits of the various proposed excitation mechanisms. Rather we attempt to develop an empirical excitation model analogous to the scheme proposed for atomic species. Harvey (1973b) has reported meteor lines of O II, Mg II, Si II, Ca II, Ti II, and Fe II in LaRC spectra. These lines in the photographic and visual parts of the spectra appear to obey the following "selection rules":

1. Only lines with *even* multiplicities of the upper states are seen.

2. Only lines with *odd* parity upper states are strong; even parity states give weaker lines.

3. The most persistent lines belong to atoms which have a relatively long-lived excited state that can readily be collisionally converted to an ionic excited state (mainly Ca, Mg, and Si) with spin and parity conservation.

4. Only those transitions whose upper state energies are approximately equal to the transition energy of a spin and parity conserving $N_2^+ \rightarrow N_2$ (or in some instances $O_2^+ \rightarrow O_2$) reaction are present.

For prediction purposes we classify the odd parity lines together into Group A and the even parity lines into Group B. Only Si II has lines from *both* groups observed in the visible region.

In the -9^m Perseid, a comparison of the Group A Si II (6347 Å) line with the Group B Si II (5978 Å) line gives $(T_{ext})_{ion}$ = 10,000 °K while 6347/5041 gives a slightly lower 8,000 °K figure. Relative to the Si II ground state these results imply that the Group A Si II lines have $(T_{ext})_A$ = 6000°K and Group B Si II lines $(T_{ext})_B$ = 4200°K. Since the Group A value is close to the kinetic temperature calculated from the ideal dissociating gas formula for a N_2 vibration temperature of 9100°K, we will use

$$(T_{ext})_A = T_{kin} = 5.9\ V_\infty^{1.7} \qquad \ldots (29)$$

where T_{kin} is derived from the relationship $T_{vib}/T_{kin} = 0.44\ (e^{T_{vib}/T_{kin}} - 1)$ with $T_{vib} = 2.5\ V_\infty^2$. Such a result is expected if the *odd* parity ionic states arise through $N_2^+ \rightarrow N_2$ collisions.

For the Group B lines, we note that the only ones observed are those with upper states which are about 12 eV above the ground state and no others.

The required energy and spin selection rules cannot be satisfied for Group B lines by $N_2^+ \rightarrow N_2$ reactions. However, dissociative recombination collisions of $O_2^+ \rightarrow 2\ O$ can satisfy the 12 eV energy constraint through several different paths as well as satisfying the spin-parity constraints. Since the numbers of O_2^+ ions must be quite small near maximum light for meteors with $V_\infty > 40$ km/sec, it seems possible to qualitatively account for the apparent lack of even parity, odd multiplicity ionic states. In this instance it appears that O_2^+ effects cannot be ignored. Since the mechanics of the O_2^+ collisions are fundamentally different from those involving N_2^+ there is no reason to expect the resulting ionic excitation temperatures to be the same.

Within the context of dissociative recombination of O_2^+, the newly produced ions retain only their original atomic temperature distribution such that

$$(T_{ext})_B = (T_{ext})_{atom}$$

with the O I products retaining the original O_2^+ energy distribution. The result for the Group B silicon lines is in accord with this hypothesis.

The above scheme is quite hypothetical and far from satisfactory and the resulting extrapolation into the ultraviolet is at best only an average since

$$(T_{ext})_{N_2^+} \geq (T_{ext})_{ions} \geq (T_{ext})_{atoms}$$

In view of the fact that most ionic lines are seen at low meteor altitudes and in mainly the brightest meteors, a detailed consideration of ionization except for the purpose of computing the depletion may not be necessary for objects in the $+5 > m_{pg} > -2$ range of interest. Certainly there is no evidence to indicate that the excitation temperatures derived can really be used to calculate the line intensities except in a relative way. However, assuming the above excitation scheme is valid the ionic/neutral lines may be combined to give at 60 km/sec

$$\log \frac{N_{II}}{N_I} = 18.1 - 21.4 \log \chi \qquad \ldots (30)$$

where χ is the ionization potential in eV.

Assuming a V_∞^4 dependence for ionization we obtain the expression

$$\log \frac{N_{II}}{N_I} = 11.0 + 4 \log V_\infty - 21.4 \log \chi \qquad \ldots (31)$$

as an appropriate velocity scaling of meteor ionization. Representative values of $\log N_{II}/N_I$ are given in Table XVIII for a number of possible meteoroid elements and velocities. In Table XIX we list the corresponding logarithmic depletion factors N_{II}/N and N_I/N where N is the elemental abundance. Since the ionic excitation temperatures may be average values, the computed depletion factors represent only lower bounds.

If the depletion factors are applied to the previously quoted preliminary abundances, values somewhat closer to the composition of an ordinary carbonaceous chondrite are obtained.

Table XVIII - Ion-Atom Ratios

Species	χ(eV)	$\log_{10}(N_{II}/N_I)$ and a V_∞^4 relationship			
		40	50	60	70
H	13.6	-6.9	-6.5	-6.2	-5.9
Be	9.3	-3.3	-2.9	-2.6	-2.3
B	8.3	-2.2	-1.8	-1.5	-1.2
C	11.3	-5.1	-4.8	-4.4	-4.2
N	14.5	-7.4	-7.0	-6.7	-6.4
O	13.6	-6.9	-6.5	-6.2	-5.9
Mg	7.6	-1.5	-1.1	-0.8	-0.5
Na	5.1	+2.5	+2.9	+3.2	+3.5
Al	6.0	+0.7	+1.1	+1.4	+1.7
Si	8.1	-2.0	-1.6	-1.3	-1.0
P	10.4	-4.4	-4.0	-3.7	-3.4
S	10.3	-4.0	-3.6	-3.3	-3.0
Ca	6.1	+0.8	+1.2	+1.5	+1.8
Ca II	11.9	-5.6	-5.2	-4.9	-4.6
Mn	7.4	-1.1	-0.7	-0.4	-0.1
Fe	7.9	-1.8	-1.4	-1.1	-0.8
Cr	6.8	-0.4	0.0	+0.3	+0.6
Ti	6.8	-0.4	0.0	+0.3	+0.6
V	6.8	-0.3	+0.1	+0.4	+0.7
Co	7.9	-1.8	-1.4	-1.1	-0.8
Ni	7.6	-1.4	-1.0	-0.7	-0.4
Cu	7.7	-1.6	-1.2	-0.9	-0.6
Zn	9.4	0.0	+0.4	+0.7	+1.0

Table XIX - Predicted Depletion Factors

	$\log_{10}(N_{II}/N)$				$\log_{10}(N_{I}/N)$			
Element	40 km/sec	50 km/sec	60 km/sec	70 km/sec	40 km/sec	50 km/sec	60 km/sec	70 km/sec
H	-6.9	-6.5	-6.2	-5.9	0.0	0	0	0
Be	-3.3	-2.9	-2.6	-2.3	0.0	0	0	0
B	-2.2	-1.8	-1.5	-1.2	0.0	0	0	0
C	-5.1	-4.8	-4.4	-4.2	0.0	0	0	0
N	-7.4	-7.0	-6.7	-6.4	0.0	0	0	0
O	-6.9	-6.5	-6.2	-5.9	0.0	0	0	0
Mg	-1.5	-1.1	-0.8	-0.6	0.0	0.0	-0.1	-0.1
Na	0	0	0	0	-2.5	-2.9	-3.2	-3.5
Al	-0.1	0.0	0.0	0.0	-0.8	-1.1	-1.4	-1.7
Si	-2.0	-1.6	-1.3	-1.0	0	0	0	0
P	-4.4	-4.0	-3.7	-3.4	0	0	0	0
S	-4.0	-3.6	-3.3	-3.0	0	0	0	0
Ca	-0.1	0.0	0.0	0.0	-0.9	-1.2	-1.5	-1.8
Ca II	-5.6	-5.2	-4.9	-4.6	0	0	0	0
Mn	-1.1	-0.8	-0.5	-0.3	0	-0.1	-0.1	-0.3
Fe	-1.8	-1.4	-1.1	-0.8	0.0	0.0	0.0	-0.1
Cr	-0.5	-0.3	-0.2	-0.1	-0.1	-0.3	-0.5	-0.7
Ti	-0.5	-0.3	-0.2	-0.1	-0.1	-0.3	-0.5	-0.7
V	-0.5	-0.3	-0.2	-0.1	-0.2	-0.4	-0.5	-0.8
Co	-1.8	-1.4	-1.1	-0.8	0	0	0	-0.1
Ni	-1.4	-1.0	-0.8	-0.5	0	0	-0.1	-0.1
Cu	-1.6	-1.2	-0.9	-0.7	0	0	0	-0.1
Zn	-0.3	-0.1	-0.1	0.0	-0.3	-0.5	-0.8	-1.0

Depletion Corrected Abundances by Number

Atom	Shower Meteor			Carbon. Chond.	Av. Shower Meteor
	Taurid	Geminid	Perseid		
Fe	1.0	1.0	1.0	1.0	1.0
Ni	1.2×10^{-1}	1.3×10^{-1}	-	5×10^{-1}	10^{-1}
Ca	4.8×10^{-4}	8.7×10^{-3}	1.9×10^{-2}	6×10^{-2}	10^{-2}
Mn	3.3×10^{-4}	4.2×10^{-4}	6.3×10^{-4}	6×10^{-3}	5×10^{-4}
Cr	5.2×10^{-4}	7.2×10^{-4}	1.5×10^{-3}	8×10^{-3}	10^{-3}
Mg	0.77	0.92	1.0	1.0	0.9
Si	2.3	2.1	2.2	1.0	2.2
Na	4.4×10^{-3}	3.6×10^{-2}	1.1×10^{-1}	3×10^{-2}	5×10^{-2}

Even with corrections for possible moderate ionic depletion it is not possible to make the meteoroid compositions come into agreement with the ordinary carbonaceous chondrites. Although a carbonaceous chondritic composition will be assumed for the computations in the next part, it should be noted that such an assumption probably *underestimates* abundances of the lighter elements by a factor of two to ten while *overestimating* the heavier elements by similar factors. The critical role ionization plays in the determination of abundances is obvious.

Text References - Part II

1. Allen, C. W.: Astrophysical Quantities. The Athlone Press, Univ. of London, 1963, p. 34.

2. Aller, L. H.: The Atmospheres of the Sun and Stars. Ronald Press, 1963, p. 439.

3. Ayers, W. G.; McCrosky, R. E.; and Shao, C.-Y.: Photographic Observations of 10 Artificial Meteors. Smithsonian Astrophy. Obs. Special Report no. 317, 1970.

4. Baker, R. M. L.: The Transitional Aerodynamic Drag of Meteorites. Astrophys. J., vol. 129, 1959, pp. 826-841.

5. Cook, A. F.: The Nature of Meteoric Radiation. Meteors, T. R. Kaiser, ed., Special Suppl. J. Atm. Terr. Phys., vol. 2, 1955, pp. 8-15.

6. _____; Jacchia, L. G.; and McCrosky, R. E.: Luminous Efficiency of Iron and Stone Asteroidal Meteors. Smithsonian Contr. Astrophy., vol. 7, 1963, pp. 209-220.

7. _____; Forti, G.; McCrosky, R. E.; Posen, A.; Southworth, R. B.; and Williams, J. T.: Combined Observations of Meteors by Image-Orthicon Television Camera and Multi-Station Radar. Evolutionary and Physical Properties of Meteoroids. NASA SP-319, 1973, pp. 23-44.

8. Ceplecha, Z.: Study of a Bright Meteor Flare by Means of Emission Curve of Growth. Bull. Astron. Inst. Czech., vol. 15, 1964, pp. 102-112.

9. _____: Spectroscopic Analysis of Iron Meteoroid Radiation. Bull. Astron. Inst. Czech., vol. 18, 1967, pp. 303-310.

10. _____: Evidence from Spectra of Bright Fireballs. Evolutionary and Physical Properties of Meteoroids. NASA SP-319, 1973, pp. 89-102.

11. Evans, J. V.: Radar Observations of Meteors. Smithsonian Contr. Astrophy., vol. 11 (NASA SP-135), 1967, pp. 133-149.

12. Friichtenicht, J. F.; and Becker, D. G.: Determination of Meteor Parameters Using Laboratory Simulation Techniques. Evolution and Physical Properties of Meteoroids. NASA SP-319, 1973, pp. 53-81.

13. Harvey, G. A.: The Calcium H and K-line Anomaly in Meteor Spectra. Astrophy. J., vol. 165, 1971, pp. 669-671.

14. _____: Elemental Abundance Determinations for Meteors by Spectroscopy. J. Geophys. Res., vol. 78, 1973a, pp. 3913-3926.

15. _____: Spectral Analysis of Four Meteors. Evolution and Physical Properties of Meteoroids. NASA SP-319, 1973b, pp. 103-129.

16. _____: Strongly Differentiated Material in High-Inclination and Retrograde Orbits. Astron. J., vol. 79, 1974, pp. 333-347.

17. _____: Analysis of Air Radiation in Photographic Meteor Spectra. J. Geophys. Res., 1976.

18. Hawkins, G. S.; and Southworth, R. B.: The Statistics of Meteors in the Earth's Atmosphere. Smithsonian Contr. Astrophys., vol. 2, 1958, pp. 349-364.

19. Hoffman, H. S.: Ionic Spectra of Meteors. Astrophys. J., vol. 163, 1971, pp. 393-403.

20. Hoffman, H. S.; and Longmire, M. S.: Meteor Ion Spectra. Nature, vol. 218, 1968, pp. 858-859.

21. Jacchia, L. G.: The Physical Theory of Meteors VIII. Fragmentation of the Faint-Meteor Anomaly. Astrophy. J., vol. 121, 1955, pp. 521-527.

22. _____; Verniani, F.; and Briggs, R. E.: Selected Results from Precision-Reduced Super-Schmidt Meteors. Smithsonian Contr. Astrophys., vol. 11 (NASA SP-135), 1967, pp. 1-7.

23. Jones, J.; and Kaiser, T. R.: The Effects of Thermal Radiation, Conduction and Meteoroid Heat Capacity on Meteoric Ablation. Mon. Not. Roy. Astron. Soc., vol. 133, 1966, pp. 411-420.

24. _____; and Hawkes, R. L.: Television Observations of Faint Meteors - II. Mon. Not. Roy. Astron. Soc., vol. 171, 1975, pp. 159-169.

25. Lebedinec, V. N.; and Portnyagin, Yu. I.: Fragmentation of Dense Meteoroids in the Atmosphere. Sov. Astron. A. J., vol. 11, 1968, pp. 700-711.

26. Lindblad, B. A.: The Relation Between Visual Magnitudes of Meteors and the Durations of Radar Echos. Smithsonian Contr. Astrophys., vol. 7, 1963, pp. 27-39.

27. McKinley, D. W. R.: Meteor Science and Engineering. McGraw-Hill, Ch. 7, 1961.

28. McCrosky, R. E.; and Soberman, R. K.: Results from an Artificial Iron Meteoroid at 10 km/sec. Smithsonian Contr. Astrophys., vol. 7, 1963, pp. 199-208.

29. Millman, P. M.: An Analysis of Meteor Spectra. Harvard Coll. Obs. Ann., vol. 82, 1932, pp. 113-146.

30. _____: An Analysis of Meteor Spectra, Second Paper. Harvard Coll. Obs. Ann., vol. 82, 1935, pp. 149-177.

31. _____: A General Survey of Meteor Spectra. Smithsonian Contr. Astrophys., vol. 7, 1963, pp. 119-127.

32. Mitchell, A. C. G.; and Zemansky, M. W.: Resonance Radiation and Excited Atoms. Cambridge Univ. Press (London), 1961, p. 101.

33. Moore, F. K.: Model of Gas Flows with Chemical and Radiative Effects. Space Mathematics - Part 3, J. B. Rosser, ed., Am. Math. Soc. (Providence, Rhode Island), 1966, pp. 94-152.

34. Morton, D. C.: Interstellar Absorption Lines in the Spectrum of Zeta Ophiuchi. Astrophys. J., vol. 197, 1975, pp. 85-115.

35. _____; and Smith, W. H.: A Summary of Transition Probabilities for Atomic Absorption Lines Formed in Low Density Clouds. Astrophys. J. Suppl., vol. 26, 1973, pp. 333-364.

36. Nicholls, R. W.; Parkinson, W. H.; and Reeves, E. M.: The Spectroscopy of Shock Excited Powdered Solids. Appl. Optics, vol. 2, 1963, pp. 919-930.

37. Rajchl, J.: A Short Note on Meteor Spectra with Low Dispersion. Smithsonian Contr. Astrophys., vol. 7, 1963, pp. 155-159.

38. _____: Some Results from Meteor Spectra of Low Dispersion. Bull. Astron. Inst. Czech., vol. 15, 1964, pp. 138-144.

39. Savage, H. F.; and Bointnott, C. A.: Laboratory Determination of the Luminous Efficiency of Meteor Constituents. Evolutionary and Physical Properties of Meteoroids. NASA SP-319, 1973, pp. 83-87.

40. Spitzer, L.: The Distribution of Interstellar Sodium. Astrophys. J., vol. 108, 1948, pp. 276-309.

41. Strömgren, B.: On the Density Distribution and Chemical Composition of the Interstellar Gas. Astrophys. J., vol. 108, 1948, pp. 242-275.

42. Tagliaferri, E.; and Slattery, J. C.: A Spectral Measurement of Simulated Meteors. Astrophys. J., vol. 155, 1969, pp. 1121-1127.

43. Verniani, F.: On Meteor Ablation in the Atmosphere. Nuovo Cimento, vol. 19, 1961, pp. 415-442.

44. _____: On the Luminous Efficiency of Meteors. Smithsonian Contr. Astrophys., vol. 8, 1964, pp. 141-172.

45. _____: Structure and Fragmentation of Meteoroids. Space Sci. Rev., vol. 10, 1969, pp. 230-261.

46. _____: An Analysis of the Physical Parameters of 5729 Faint Radio Meteors. J. Geophys. Res., vol. 78, 1973, pp. 8429-8462.

47. _____; and Hawkins, G. S.: On the Ionizing Efficiency of Meteors. Astrophys. J., vol. 140, 1964, pp. 1590-1600.

48. Weast, R. C.: Handbook of Chemistry and Physics. 51st ed. Chemical Rubber Co. (Cleveland, Ohio), 1970.

49. Whitten, R. C.; and Poppoff, I. G.: Fundamentals of Aeronomy. John Wiley and Sons, 1971.

50. Wilson, O. C.; and Merrill, P. W.: Analysis of the Intensities of the Interstellar D Lines. Astrophys. J., vol. 86, 1937, pp. 44-69.

Part III. Computation of Synthetic Ultraviolet Meteor Spectra of Carbonaceous Chondritic Composition.

In this part, the excitation theory developed in Part II will be used to predict the ultraviolet spectrum for cases which have the greatest potential for satellite detection.

The excitation relations for a meteor at average incidence ($\cos \theta = 0.67$) become

$$(T_m)_I = 152\ V_\infty^{0.8}\ e^{-8.7 \times 10^{-3}(H_m - H_{Fe})} \quad \ldots (1)$$

$$T_A = 2.5\ V_\infty^2\ ,\ T_{kin} = 5.9\ V_\infty^{1.7} \quad \ldots (2)$$

$$\log_{10} \frac{N_{II}}{N_I} = 11.0 + 4 \log_{10} V_\infty - 21.8 \log_{10} \chi(eV) \quad \ldots (3)$$

$$(T_m)_{II} = T_{kin} \text{ (Group A - } N_2^+ \rightarrow N_2 \text{ reactions)} \quad \ldots (4)$$

$$(T_m)_{II} = (T_m)_I \text{ (Group B - } O_2^+ \rightarrow O_2 \text{ reactions)} \quad \ldots (5)$$

Here $(T_m)_I$ is the meteor atomic excitation temperature, $(T_m)_{II}$ is the meteor ionic excitation temperature, T_A is the air excitation temperature, T_{kin} is the air dissociation or kinetic temperature, N_{II} is the ionic density, N_I is the neutral species, V_∞ is the geocentric meteor velocity in km/sec, H_m is the heat of vaporization at 25°C for the particular meteoric element (or the bond strength for molecules) and H_{Fe} is the heat of vaporization of iron at 25°C, and χ(eV) is the ionization potential in electron volts.

For the standard abundance, the ordinary carbonaceous chondrite has been selected (Mason, 1962). The gf values for the selected UV lines of the synthetic spectra have been taken from Morton and Smith (1973); Morton (1975); Kurucz (1974) and where the partition functions are from Allen (1963). Excitation potentials were taken from Moore (1968). Using expression (3) above gives the atomic and ionic abundances listed in Table XX. These values are automatically corrected for depletion. The calculations at 40 km/sec, 50 km/sec, 60 km/sec, and 70 km/sec approximate the velocities of major objects of interest. Except for the Leonids at maximum light, the reference heights at each velocity are considered to be identical for all objects. For the Leonids the height of maximum light is 10 km lower than for other 70 km/sec meteoroids so that their far UV lines must be computed separately. For N I, O I, and H I line absorption calculations, the T_{kin} has been adopted as the plasma temperature giving the meteor line doppler broadening.

Table XX - Atomic and Ionic Abundances Assuming a Carbonaceous Composition and as a Function of Velocity

Element	Car. Chon. $\log_{10}N$	$\log_{10}N_I$ Velocity (km/sec)				$\log_{10}N_{II}$ Velocity (km/sec)			
		40	50	60	70	40	50	60	70
H	7.0	7.0	7.0	7.0	7.0	+0.1	+0.5	+0.8	+1.1
Be	2.8	2.8	2.8	2.8	2.8	-0.5	-0.1	+0.2	+0.5
B	2.8	2.8	2.8	2.8	2.8	+0.6	+1.0	+1.3	+1.6
C	6.4	6.4	6.4	6.4	6.4	+1.3	+1.6	+2.0	+2.2
N	5.8	5.8	5.8	5.8	5.8	-1.6	-1.2	-0.9	-0.6
O	6.7	6.7	6.7	6.7	6.7	-0.2	+0.2	+0.5	+0.8
Mg	7.5	7.5	7.5	7.4	7.4	+6.0	+6.5	+6.7	+6.9
Na	6.1	3.6	3.2	2.9	2.6	+6.1	+6.1	+6.1	+6.1
Al	6.4	5.6	5.3	5.0	4.7	+6.3	+6.4	+6.4	+6.4
Si	7.5	7.5	7.5	7.5	7.5	+5.5	+5.9	+6.2	+6.5
P	5.5	5.5	5.5	5.5	5.5	+1.5	+1.5	+1.8	+2.1
S	7.4	7.4	7.4	7.4	7.4	+3.4	+3.8	+4.1	+4.4
Ca	6.4	5.3	5.2	4.9	4.6	+6.3	+6.4	+6.4	+6.4
Mn	5.3	5.3	5.3	5.2	5.1	+4.2	+4.5	+4.8	+5.1
Fe	7.5	7.5	7.5	7.5	7.4	+5.7	+6.1	+6.4	+6.7
Cr	5.5	5.4	5.2	5.0	4.8	+5.0	+5.2	+5.3	+5.4
Ti	5.5	5.4	5.2	5.0	4.8	+5.0	+5.2	+5.3	+5.4
V	5.5	5.3	5.1	5.0	4.7	+5.0	+5.2	+5.3	+5.4
Co	4.9	4.9	4.9	4.9	4.9	+3.1	+3.5	+3.8	+4.1
Ni	6.2	6.2	6.2	6.1	6.1	+4.8	+5.2	+5.4	+5.7
Cu	4.5	4.5	4.5	4.5	4.4	+2.9	+3.3	+3.6	+3.8
Zn	4.5	4.0	3.8	3.5	3.3	+4.0	+4.3	+4.2	+4.3

Table XXI -
Excitation and Ionization Properties
of Synthetic Spectrum Models

V_∞ (km/sec)	H_o' (km)	Objects of Model Representation	T_{Fe}	T_{Air}	T_{kin}	$21.8 \log \chi_{10} + \log_{10}\left(\frac{N_{II}}{N_I}\right)$
40	90	Mean shower & sporadic	2900	4000	3100	17.4
50	97	Lyrids	3500	6200	4600	17.8
60	100	Perseids	4000	9000	6200	18.1
70	100	Beginning Leonids, Orionids, η Aqr	4600	12000	8000	18.4
70	90	Maximum Light Leonids	4600	12000	8000	18.4

In order to get some idea of what a UV meteor spectrum might look like, the lines of greatest oscillator strength and/or lowest excitation potential were selected.

The results for neutral species are presented in Table XXII where all intensities are given relative to the Fe I 3720 line intensity. If we take a line width appropriate to the kinetic temperature of the meteor (~5000°K) the relative line intensities can be converted to fluxes using the following approximate calibration curves for the peak intensities

$$\log \eta \text{ (photons/cm}^2\text{-sec)} = \log (I_\lambda / I_{3720}) + 2.5 + \log \lambda \text{ (Å)} - 0.4\, M_{pg} \quad \ldots (6)$$

$$\log E \text{ (ergs/cm}^2\text{-sec-Å)} = \log (I_\lambda / I_{3720}) - 5.2 - 0.4\, M_{pg} \quad \ldots (7)$$

where M_{pg} is the photographic absolute magnitude of the meteor.

For the ionic UV lines only the transitions satisfying the selection rules (Part II) were considered. The results were normalized to the Ca II 3933 line. Transitions which had log (I_λ / I_{3933}) larger than -8.0 are given in Table XXIII. The approximate flux calibrations for the ions are given by

$$\log \eta' \text{ (photons/cm}^2\text{-sec)} = \log (I_\lambda / I_{3933}) + 1.1 - 0.5\, M_{pg} \quad \ldots (8)$$

and

$$\log E' \text{ (ergs/cm}^2\text{-sec)} = \log (I_\lambda / I_{3933}) - 6.6 - 0.5\, M_{pg} \quad \ldots (9)$$

Corrections for O_2 attenuation have been applied where necessary.

As was indicated earlier, the predictions for molecular species survival and excitation is very uncertain. For lack of a better model, it was assumed that (except for OH where an initial composition of H_2O was used) the molecular abundance was equal to the atomic abundance of the most abundant atom in the molecule. Furthermore it was assumed that the molecular excitation temperature could be obtained from the previously derived heat-of-vaporization correlation by simply substituting the molecular heat of formation for the heat of vaporization. In Table XXIV we give the results for several molecules of interest normalized to the atomic Fe I 3720 line. Corrections for O_2 atmospheric attenuation have been included where necessary. Once a direct calibration for the OH 3090 intensity becomes available, a renormalization of the molecular intensities will be possible and perhaps a better extrapolation to the far-ultraviolet region can be calculated. Until then a calibration using (6) or (7) is the best approach.

Table XXII - Predicted Relative Intensities of Selected Neutral Atom Species in the Ultraviolet

λ	Species	log (I_{line}/I_{3720}) at average incidence				
		40 km/sec	50 km/sec	60 km/sec	70 km/sec	Leonid
1025	H I	-3.1	-1.9	-1.1	-0.7	-1.4
1200	N I	-4.0	-3.1	-2.5	-2.0	-2.6
1216	H I	-1.5	-0.6	+0.0	+0.2	+0.1
1302-4	O I	-4.3	-2.4	-2.4	-1.5	-2.1
1330	C I	-17.9	-14.6	-12.4	-11.1	-11.6
(1330)*	C I	-8.4	-6.7	-5.7	-5.0	-5.5
1425	S I	-4.9	-3.3	-2.3	-1.9	-2.7
1433	S I	-5.2	-3.6	-2.6	-2.2	-3.0
1561	C I	-16.8	-12.5	-10.2	-9.1	-11.7
(1561)*	C I	-8.2	-5.8	-4.1	-4.0	-6.6
1657	C I	-15.3	-11.3	-9.1	-8.1	-10.7
(1657)*	C I	-7.7	-4.9	-3.6	-3.2	-5.8
1672	P I	-3.5	-2.4	-1.4	-1.7	-2.4
1675	P I	-3.1	-2.0	-1.1	-1.3	-2.1
1680	P I	-3.0	-2.0	-1.0	-1.3	-2.1
1775	P I	-2.9	-2.2	-1.3	1.7	-2.1
1807	S I	-2.0	-1.3	-0.9	-0.6	-0.7
1820	S I	-2.3	-1.7	-1.2	-0.9	-1.0
1936	Al I	-3.6	-3.4	-2.5	-3.4	-3.4
2094	Cr I	-7.2	-6.7	-6.3	-5.8	-5.8
2138	Zn I	-1.5	-1.6	-1.5	-2.0	-2.0
2269	Al I	-3.0	-2.9	-2.9	-3.0	-3.0
2349	Be I	-4.1	-3.8	-3.6	-3.4	-3.4
2373	Al I	-2.5	-2.5	-2.6	-3.0	-3.0
2483	Fe I	-1.6	-1.1	-0.7	-0.6	-0.6
2498	B I	-7.3	-6.6	-6.2	-5.9	-5.9
2516	Si I	-3.0	-2.5	-2.0	-1.8	-1.8
2523	Fe I	-1.7	-1.3	-0.7	-0.7	-0.7
2619	Ti I	-5.6	-5.4	-5.1	-5.3	-5.3
2653	Al I	-3.6	-3.4	-2.3	-3.4	-3.4
2660	Al I	-2.6	-2.7	-2.8	-3.1	-3.1
2719	Fe I	-1.4	-1.1	-0.8	-0.6	-0.6
2722	Ca I	+0.0	-0.5	-0.8	-1.2	-1.2
2795	Mn I	-1.1	-1.1	-1.1	-1.2	-1.2
2798	Mn I	-0.6	-0.6	-0.6	-0.8	-0.8
2801	Mn I	-0.8	-0.9	-0.8	-1.0	-1.0
2852	Mg I	+3.6	+3.3	+3.3	+3.1	+3.1
2853	Na I	-3.5	-4.2	-4.5	-4.9	-4.9
2967	Fe I	-1.0	-0.6	-0.5	-0.4	-0.4
2973	Fe I	-1.2	-0.9	-0.7	-0.6	-0.6
3021	Fe I	-1.8	-1.0	-0.8	-0.7	-0.7
3044	Co I	-4.0	-3.8	-3.6	-3.5	-3.5

*Computed assuming all carbon is in volatile hydrocarbon form.

Table XXII (continued)

λ	Species	log (I_{line}/I_{3720}) at average incidence 40 km/sec	50 km/sec	60 km/sec	70 km/sec	Leonid
3185	V I	-2.6	-2.7	-2.5	-3.0	-3.0
3226	V I	-5.3	-5.4	-5.2	-5.7	-5.7
3247	Cu I	-1.2	-1.2	-1.2	-1.3	-1.3
3371	Ti I	-2.7	-2.8	-3.0	-3.1	-3.1
3415	Ni I	-1.5	-1.4	-1.3	-1.3	-1.3
3524	Ni I	-1.3	-1.2	-1.1	-1.2	-1.2
3527	Co I	-3.3	-3.3	-3.2	-3.2	-3.2
3578	Cr I	-1.5	-1.7	-1.7	-2.0	-2.0
3720	Fe I	+0.0	+0.0	+0.0	+0.0	+0.0

Table XXIII - Predicted Ionic Relative Logarithmic Intensities in UV Meteor Spectra

		log (I_λ / I_{3933})				
λ	Species	40 km/sec	50 km/sec	60 km/sec	70 km/sec	Leonids
1670	Al II	-7.4	-4.0	-1.7	-0.6	-2.6
2343	Fe II	-6.3	-4.7	-3.4	-3.0	-3.0
2382	Fe II	-5.5	-4.1	-3.2	-2.4	-2.4
2576	Mn II	-7.4	-6.3	-5.1	-4.8	-4.8
2599	Fe II	-5.3	-4.3	-3.4	-2.8	-2.8
2701	V II	-6.7	-5.8	-5.2	-4.8	-4.8
2795	Mg II	-2.2	-1.6	-1.0	-0.5	-0.5
2803	Mg II	-3.2	-2.0	-1.4	-0.9	-0.9
2910	Ti II	-8.3	-7.5	-7.0	-6.7	-6.7
3933	Ca II	0.0	0.0	0.0	0.0	0.0

Table XXIV - Predicted Molecular Relative Logarithmic Intensities in UV Meteor Spectra

λ	Species	log (I_λ/I_{3720}) 40 km/sec	50 km/sec	60 km/sec	70 km/sec	Leonids
1088	CO	-15.4	-12.1	-10.2	-8.4	-9.2
1151	CO	-14.7	-12.0	-10.2	-8.6	-9.0
1194	H_2O	-12.7	-10.0	-8.5	-7.0	-7.5
1222	OH	-12.6	-9.4	-8.1	-6.5	-7.3
1240	H_2O	-12.4	-9.7	-8.2	-6.7	-7.2
1310	SiO	-3.7	-3.2	-2.5	-2.1	-2.6
3090	OH	-3.4	-3.1	-2.8	-2.5	-2.5
3140	CH	-2.9	-2.6	-2.4	-2.1	-2.1

Part IV. Summary and Recommendations

A. Expected Nature of the UV Radiation.

Now that at least one model of UV meteor emission has been calculated, the somewhat vague experimental suggestions of the interviewed meteor scientists can be cast into a more definitive form.

It is indicated from the calculations presented in Part III that the predicted ultraviolet emission is somewhat weaker than was originally hoped. However, because UV detectors are generally more efficient than those available for the photovisual spectral regions, this reduction in intensity is not considered serious.

To briefly summarize the results of Part III, the dominant line(s) for the elements of greatest interest are given with relative qualitative strengths (S = strong, M = moderate, W = weak and U = probably not observable).

Element	λ(Å)	Prob. Strength	El./Ion/Mole.	λ(Å)	Prob. Strength
H	1216	S	Ti	3371	W
	1025	M	V(*)	3185	W
Be(*)	2349	W	Cr	3578	M
B(*)	2498	U	Mn	2798	S
C(*)	1657	U to W	Fe	2967	S
N	1200	W	Co	3527	W
O	1304	W	Ni	3524	M
Na	2853	W	Cu(*)	3247	M
Mg	2852	Very S	Zn(*)	2138	M
Al	1936	W	Al II	1670	M
	2653	M	Fe II	2343,2382	M
Si	2516	M	Mg II	2795,2803	S
P(*)	1680	S	SiO	1310	W
S(*)	1807	S	OH	3090	W
Ca	2722	S	CH	3140	W

*Element not yet found in meteor spectra.

Except for boron (which was not expected to be detectable anyway) sodium, and carbon it appears that most elements of interest have at least one line that might provide abundance information from a UV meteor spectrum.

Since the atmospheric contribution to the N I and O I emission is expected to be considerable it is unlikely that observations of the 1200 Å and 1304 Å lines will give meteoroid information. For 1304 Å, SiO emission may be bothersome.

From an instrumental and detection standpoint it probably is more useful to arrange the information in wavelength groups.

Far Ultraviolet Region (λ < 2000 Å)

H	1216,1025	S	P	1680	S
C	1657	U to W	S	1807	S
N	1200	W	Al II	1670	M
O	1304	W	SiO	1310	W
Al	1936	W			

Middle Ultraviolet Region (3000 Å > λ > 2000 Å)

Be	2349	W	Ca	2722	S
B	2498	U	Mn	2798	S
Na	2853	W	Fe I	2967	S
Mg	2852	Very S	Zn	2138	M
Al	2653	M	Fe II	2343,2382	M
Si	2516	M	Mg II	2795,2803	S

Near Ultraviolet Region (3600 Å > λ > 3000 Å)

Ti	3371	W	Ni	3524	M
V	3185	W	Cu	3247	M
Cr	3578	M	OH	3090	W
Co	3527	W	CH	3140	W

Because the detection of carbon was often mentioned as desirable by a number of the workers in meteor physics consulted during this study, it was quite disappointing to find the extremely low elemental heat of vaporization capable of preventing observable excitation. Although sufficient atomic oxygen is present in the meteor plasma to produce CO in reasonable amounts, this molecule appears to be virtually undetectable also because of the extremely high excitation temperatures required. Calculations of the ionized carbon line strengths were similarly disappointing. Only if a sizeable fraction of the meteoroid carbon is tied up in hydrocarbons rather than oxides or graphitic forms does there appear to be a chance of spectroscopic detection. Indeed, the calculations suggest that if there were a *positive* detection of meteoric CH at 3140 Å, then a search for C I 1657 would seem more worthwhile.

Reference to Table I (Part I) indicates the spectroscopic contamination expected for each line listed above. As is the case for fast meteor photographic spectra, air N_2 emission is very likely to be quite bothersome in any spacecraft experiment. Because of dissociation when V_∞ > 40 km/sec, the listed O_2 bands are not expected in emission except possibly in the meteor wake.

B. Major Problems in Meteor Physics.

For purposes of experiment definition, the problems connected with the determination of meteoroid elemental abundances fall into four areas (Harvey, 1973a).

A. Vaporization and Excitation
B. Ionization and Ionic Depletion
C. Dissociation and Molecular Depletion
D. Line Saturation Effects

The availability of UV meteor spectra could contribute significantly in all four areas. For example, the proposed heat-of-vaporization and excitation correlation could easily be tested by comparing the Si excitation temperature derived from the Si 2516/2216 ratio or the Fe excitation temperature with the Mg excitation temperature obtained from the 2026/2852 ratio. Significant information about ionization processes and depletion could be obtained by comparing Mg I 2852 to Mg II 2795; Al I 2653 to Al II 1670; and Fe I 2967 to Fe II 2343.

Comparison of the SiO 1310 emission to the Si I 2516 line along with measurements of the OH 3090 and CH 3140 bands can be expected to yield information on the role of molecular depletion and the extent of molecular dissociation during sputtering. Finally observation of the relative intensities of the Fe I lines in the 2000-3000 Å region compared to Mg II 2795/2803; Al I 2652/2660; P I 1774/1783/1788; S I 1900.3/1915 should settle once and for all the present controversy over line saturation effects.

Extension of meteor detection and study into the region of 2000-3000 Å which is largely inaccessible to ground-based observation because of ozone absorption and Rayleigh scattering seems quite *critical to meteor physics in general as well as necessary for a satisfactory resolution of the meteoroid light elemental abundance problem.* Except for detection of the carbon lines, the extension of observations into the far-ultraviolet seems to be technically feasibile at relatively low cost and with state-of-the-art equipment.

C. Detectability of Meteor Events.

As can be seen from Table IX, only Ly α and O I contribute to the discrete nightglow in the UV. But a major uncertainty in the detection of meteor events against the dark side of the earth is the UV night sky continuum exclusive of atomic and molecular lines. Two estimates, however, can be made which are in fair agreement. First if one assumes a constant photon number spectrum below 3200 Å, extrapolation of values quoted by Allen (1963) gives

$$I_{\lambda}(\text{cont.})_{\text{sky}} \geq \frac{5 \times 10^{-4}}{\lambda(\text{Å})} \text{ ergs } s^{-1}\text{Å}^{-1}\text{cm}^{-2} \text{ sterad}^{-1}$$

On the other hand the spectra presented by Fastie (1963) with appropriate corrections for spectral smearing implies that

$$I_\lambda(\text{cont.})_{\text{sky}} \leq \frac{2 \times 10^{-3}}{\lambda(\text{Å})} \text{ ergs } s^{-1}\text{Å}^{-1}\text{cm}^{-2}\text{sterad}^{-1}$$

For simplicity, the following is adopted as an average for the UV sky fog contribution incident on the front stop of each instrument

$$I_\lambda(\text{cont.})_{\text{sky}} \simeq \frac{10^{-3}}{\lambda(\text{Å})} \text{ ergs } s^{-1}\text{Å}^{-1}\text{cm}^{-2}\text{sterad}^{-1}$$

and over a 20° field of view

$$I_\lambda'(\text{cont.})_{\text{sky}} \simeq \frac{5 \times 10^{-5}}{\lambda(\text{Å})} \text{ ergs } s^{-1}\text{Å}^{-1}\text{cm}^{-2}\text{sterad}^{-1}$$

To demonstrate the feasibility of UV meteor detection from spacecraft we consider two hypothetical but nominal spectroscopic systems--one photographic and one photoelectric as compiled from manufacturers data sheets.*

Photographic System	Photoelectric System
f/2, 100 mm lens 20° field Objective grating 600 1/mm 20μ film resolution Density = 0.6 requires 10^{-7} ergs $s^{-1}\text{Å}^{-1}\text{cm}^{-2}$ λ = 1800 Å (special emulsion)	$\frac{S}{N}$ = 10 detection requires 1.2×10^{-7} ergs $s^{-1}\text{cm}^{-2}$ Filter with 20% central transmission with Gaussian shape Field limited to 20° Current Amplification 10^6 λ = 1800 Å (at peak sensitivity)

For spectral line detection from meteors these systems have comparable sensitivities such that

$$\log\left(\frac{I_\lambda}{I_{3720}}\right)_{\text{min}} = 0.4\, M_{pg} - 2.1 \qquad \lambda < 3000 \text{ Å}$$

becomes a useful estimate of performance. With a state-of-the-art electronographic camera system and the photoelectric system operated at 10^7 it might be possible to reach (I_λ/I_{3720}) values ten times fainter than given by the above formula.

While it is possible that future developments will permit gains of up to 10 above that predicted by the above equation, it is sufficiently pessimistic to use state-of-the-art parameters.

*Eastman Kodak, "Plates and Films for Scientific Photography", (1973) p. 315, Rochester, New York and EMR Photoelectric, P. O. Box 44, Princeton, N.J. 08540.

The sky brightness limiting for these systems can be expressed by the following expressions.

Photographic Skylimiting (20° field of view)

Exposures should be such that

$$t(\text{sec}) \lesssim 2 \times 10^3 \left(\frac{\lambda(\text{Å})}{\Delta\lambda(\text{Å})} \right) \qquad \text{(Excluding L}\alpha \text{ and O I 1304 Å)}$$

where λ is the mean wavelength of the instrumental bandpass and $\Delta\lambda$ is the bandpass of the emulsion (and filter if used) system.

Photoelectric Skylimiting (20° field of view)

$$\tau(\text{sec}) \lesssim 30 \frac{\lambda(\text{Å})}{\delta\lambda(\text{Å})} \qquad \text{(Excluding L}\alpha \text{ and O I 1304 Å)}$$

where $\delta\lambda$ is the required filter bandwidth and τ is the integration time.

It is assumed that both t(sec) and τ(sec) will both be longer than the meteor duration which is typically on the order of 2×10^{-1} to 5×10^{-1} seconds.

If the bandpass includes one of the bright nightglow emission lines, then the sky fog level is reached much sooner.

$$t(\text{sec}) \lesssim \frac{1}{1.5\ I_i(\kappa R)\Phi_i(\lambda)} \qquad \text{(photographic skylimiting dominated by line emission)}$$

where I_i is the line emission in kilorayleighs and Φ_i is the normalized instrumental transmission relative to the peak sensitivity.

$$\tau(\text{sec}) \lesssim \text{meteor duration} \qquad \text{(photoelectric skylimiting dominated by line emission)}$$

but now the intensity limit is

$$\log \left(\frac{I_\lambda}{I_{3720}} \right)_{\min} = 0.4\ M_{pg} + 1.0 + \log I_i(\kappa R) + \log \Phi_i(\lambda) \quad , \quad \lambda < 3000\ \text{Å}$$

where it is assumed that the filter bandwidth is wider than the meteor or airglow line width and that the meteor line for which detection is desired is *not* identical with the airglow.

D. Additional Complications in Spacecraft Observation of Meteors.

1) In the case of H I, O I, and N I where atmospheric absorption is considerable, the Doppler effect of meteor and spacecraft relative motion will

produce apparent line-strength variations that are unrelated to the abundance problem.

2) The strength of atmospheric N_2 emission may be particularly significant in the UV for fast meteors. Some degree of meteor radiation, air radiation separation should be incorporated in any experimental design. Some method of sky background and slow event discrimination would also seem to be advantageous. In particular, the meteor itself is a moving point source, the meteor wake is a line source, and the sky background is a uniform extended source. Since each of these has a distinctive Fourier transform pattern as well as time history, it should be possible to incorporate some mode of image discrimination into the spacecraft instrumentation and/or data reduction scheme to deal with this problem (Gee, Allen, and Clifton, 1973).

3) Because of spacecraft velocities up to 5 km/sec perpendicular to the earth-pointing field of view, the "diurnal" aberration of meteor positions will be much greater than is encountered in ground-based observations. One important effect will be pronounced apparent path curvature at slower meteor velocities. In addition, the aspect of any long-enduring train will be constantly shifting so that if imaging is available, stereoscopic reductions can be used to ascertain a three-dimensional trajectory. Since time-resolution is necessary to determine the meteor velocity, photographic instruments should be equipped with rotating shutters. Instrumentation with digitized readout, of course, automatically has the necessary time reference data.

E. Instrumentation Options.

Experiments suggested by meteor scientists consulted during the course of this study covered the following:

1) Broadband UV photometry
2) Narrowband UV photometry of selected features
3) Moderate to high resolution spectrophotometry in the UV
4) Laboratory studies.

Experiments in the first category are, of course, very crude but since it is of interest to obtain a direct measurement of meteor UV emission below the 3000 Å atmospheric cutoff, it seems worthwhile to propose a few meteor searches during favorable showers using existing orbiting facilities. Such an experiment, if an appropriate spacecraft is already in orbit, would be quite inexpensive compared with launching a new satellite. A comparison of the UV meteor light curve at high time resolution with those in other spectral regions might shed some light on the possible role of photoionization in the head-echo phenomenon.

Experiments in the second category represent the next degree of sophistication. Using the formula in Section C and Tables XXII, XXIII, and XXIV a number of candidate transitions can be selected. Table I indicates what difficulties will be encountered in the spectral interpretation of signals in the channels selected. The photoelectric method seems to be well-suited to

working in certain regions of the far-UV where the chances of unwanted contamination are much less. The model calculations indicate that photoelectric monitoring of 1310 Å, 1561 Å, 1807 Å, and 1936 Å should be considered. A monitoring of the 1650-1700 Å region which will be a mixture of P I, C I, and Al II does not seem to be suitable for filter photometry. Although a photoelectric photometry experiment is much simpler in concept, actual success in the meteor problem will probably depend on the maximum possible photomultiplier gain and just how narrow and efficient UV filters can be made. A multi-element detector assembly behind a simple imaging device could provide additional spatial discrimination without much additional experimental complication. Preliminary experiments to measure selected features in the near-UV should be continued to better evaluate the limitations of the photoelectric method as well as attempt the detection and interpretation of OH and CH in meteors.

Because of airglow H I and O I, the 1215 Å and 1304 Å regions are not suitable for photoelectric filter monitoring without imagery.

The most sophisticated meteor experiments discussed with various consultants involve obtaining moderate or high dispersion, spatially resolved spectra. The undeniable success of the LaRC Faint Meteor Patrol using relatively small format cameras and objective prisms and gratings provides a sound instrumental basis upon which spacecraft designs could be based. Obtaining photographic spectra down to about 2500 Å presents few technological uncertainties. Below 2500 Å, special materials to circumvent emulsion absorption problems are required, but these have been used in other spacecraft experiments and are available on special order. Electronographic cameras with vidicon readouts are much more costly but they provide real-time readout and do not require retrieval. The electronographic approach does offer the possibility of future improvement in gain over the straight photographic techniques. Spatial resolution as well as spectral resolution is required for the positive detection of meteoric H I and O I above terrestrial airglow. Unambiguous separation in crowded regions obviously require spectral and spatial resolution. Although extension of imaging down to 1500 Å involves additional expense and trouble, the expected scientific results are considerable--an understanding of meteor excitation and ionization; possible discovery of three previously undetected meteoroid elements; and the ability to derive light element abundances. A rotating shutter (or its electronic equivalent for image-intensified or electronographic devices) is suggested although it may involve higher costs and more technical problems.

Finally laboratory experiments in direct support of any UV meteor programs should include

1. Instrumentation degradation studies;

2. Derivation of additional excited state oscillator strengths of the light elements;

3. Construction of elemental emission line curves of growth using Copernicus telescope and other astronomical results where light element excitation is not a problem;

4. Continuation of ground-based, two-station meteor photography and spectroscopy with emphasis on the velocity-orbit-composition-spectra correlation problem;

5. Additional research into emission line saturation with emphasis on the doublet method; and

6. Additional research into the molecular species problem including ground-based searches for plausible species and theoretical-experimental studies of the small particle sputtering problem.

Acknowledgements

Although the contents of this report are solely the responsibility of the author, there are a number of people who contributed their time and interest to the author's perception of various aspects of the UV meteor problem and these are hereby gratefully acknowledged.

Thanks are due to Gale A. Harvey of NASA Langley Research Center for many critical discussions with regard to existing meteor spectra; to Chet B. Opal of the Naval Research Laboratory for consultation and unpublished material on the atmospheric extinction problem; to Larry Helfer of the University of Rochester, C.E.K. Mees Observatory for useful discussions and suggestions regarding the line saturation problem; to Peter Millman, B. A. McIntosh and others of the Planetary Sciences Section Herzberg Institute of Astrophysics of The National Research Council of Canada at Ottawa for useful discussions of UV detection and the head-echo problem; to Richard McCrosky and others at the Smithsonian Astrophysical Observatory for consultations regarding the UV meteor detection problem and spectral experiment interpretation; to Allan Cook of Wellesley, Massachusetts for discussions of problems connected with meteor model calculation; to D. C. Morton, W. H. Smith, and T. P. Snow of Princeton University Observatory for discussions of oscillator strengths, interstellar curves-of-growth for the light elements, line saturation problems, and examination of unpublished Copernicus data; to Z. Ceplecha of the Astronomical Institute at Oudrejov, Czechoslovakia for a comprehensive set of reprints; to Richard Madagan of Eastman Kodak Laboratories foı information concerning photographic materials available for use in the far ultraviolet; and to Judy Worden for painstaking typing of the report manuscript throughout its entire evolution.

Text References - Parts III and IV

1. Allen, C. W.: Astrophysical Quantities. The Athlone Press, Univ. of London, 1963.

2. Eastman Kodak: Kodak Plates and Films for Scientific Photography. Eastman Kodak Co. (Rochester, New York), 1974.

3. Fastie, W. G.: Instrumentation for Far-Ultraviolet Rocket Spectrophotometry. J. Quan. Spectros. Radiat. Trans., vol. 3, 1963, pp. 507-518.

4. Gee, T. H.; Allen, C. W.; and Clifton, K. S.: Application of Coherent Optical Matched Filtering for Detection of Meteor Trails. Holography and Optical Filtering. NASA SP-299, 1971, pp. 145-148.

5. Kurucz, R. L.: Semi-empirical Calculation of gf Values, III: Interstellar Lines of the Iron Group. Smithsonian Astrophys. Obs. Special Report no. 360, 1974.

6. Mason, B.: Meteorites. John Wiley and Sons, 1962.

7. Moore, C. E.: An Ultraviolet Multiplet Table. Reprint of N.B.S. Circular 488, Section 1 (1950), Section 2 (1952).

8. Morton, D. C.; and Smith, W. H.: A Summary of Transition Probabilities for Atomic Absorption Lines Formed in Low Density Clouds. Astrophys. J. Suppl., vol. 26, 1973, pp. 333-363.

9. Todd, H. N.; and Zakia, R. D.: Photographic Sensitometry. Morgan and Morgan, Inc. (Hastings-on-Hudson, New York), 1969.

10. Wood, F. B.: Astronomical Photoelectric Photometry. American Assn. for Advancement of Science (Washington, D. C.), 1953.

General References

1. Allen, C. W.: Astrophysical Quantities. The Athlone Press, Univ. of London, 1963.
2. Evolutionary and Physical Properties of Meteoroids. NASA SP-319, 1973.
3. Green, A. E. S.: The Middle Ultraviolet: Its Science and Technology. John Wiley and Sons, 1966.
4. Kresák, L.; and Millman, P. M.: Physics and Dynamics of Meteors. D. Reidel Publ. Co. (Dordrecht-Holland), 1968.
5. Koller, L. R.: Ultraviolet Radiation. John Wiley and Sons, 1965.
6. McKinley, D. W. R.: Meteor Science and Engineering. McGraw-Hill, 1961.
7. Meteor Orbits and Dust. Smithsonian Contr. Astrophys., vol. 11, 1963. (Same as NASA SP-135)
8. Millman, P. M.; and McKinley, D. W. R.: Meteors. The Moon, Meteorites, and Comets. The Solar System, vol. IV, Univ. of Chicago Press, 1963.
9. Proceedings of the Symposium on the Astronomy and Physics of Meteors. Smithsonian Contr. Astrophys., vol. 7, 1963.
10. Zaidel, A. N.; and Shreider, E. Ya. (trans. by Z. Lerman): Vacuum Ultraviolet Spectroscopy. Ann Arbor-Humphrey Science Publishers, 1970.

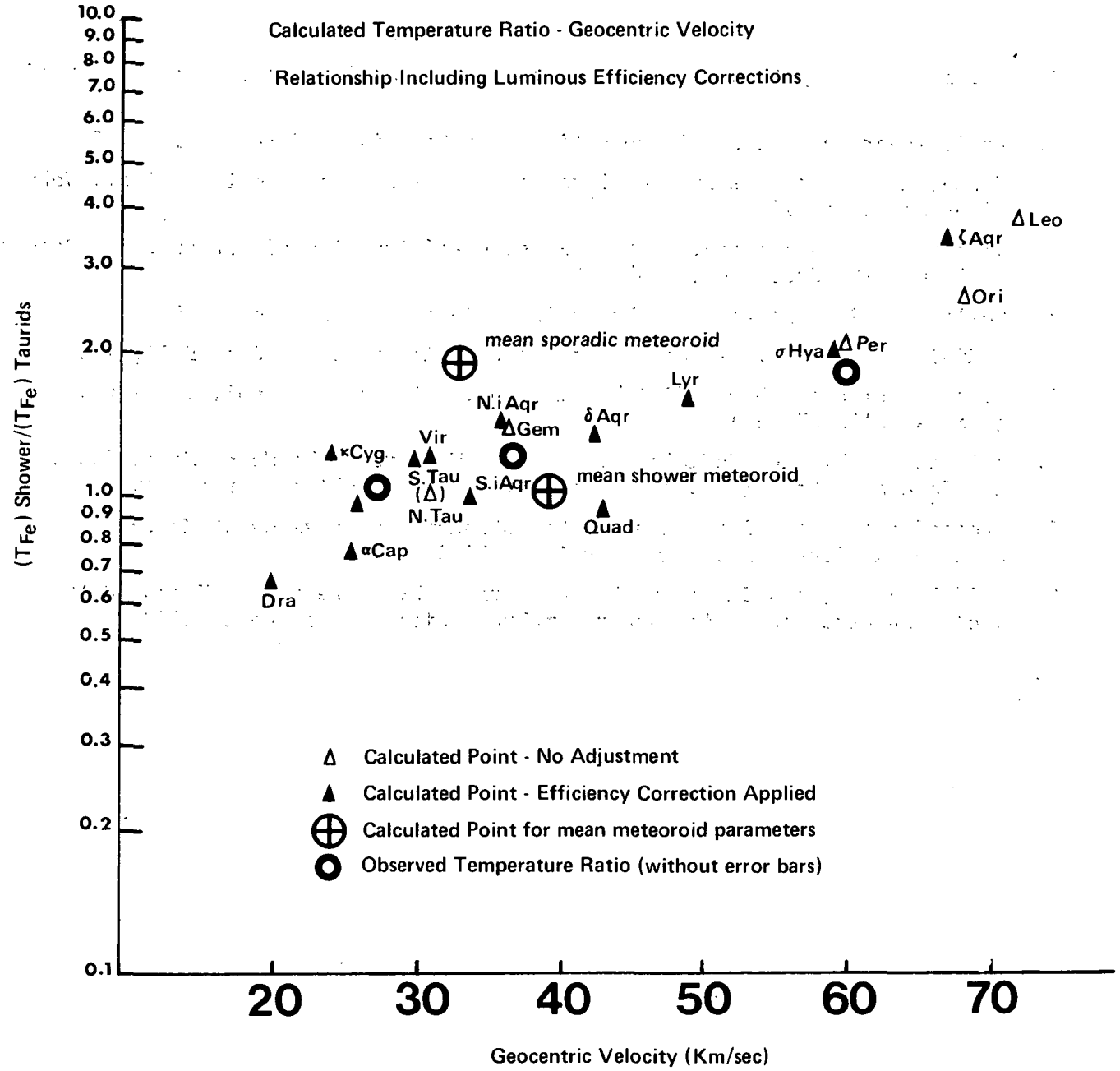
Calculated Temperature Ratio - Geocentric Velocity
Relationship Including Luminous Efficiency Corrections
(TFe) Shower/(TFe) Taurids
10.0
9.0
8.0
7.0
6.0
5.0
4.0
3.0
2.0
1.0
0.9
0.8
0.7
0.6
0.5
0.4
0.3
0.2
0.1
mean sporadic meteoroid
ΔLeo
ζAqr
ΔOri
σHya
ΔPer
Lyr
N.iAqr
δAqr
ΔGem
Vir
κCyg
S.Tau
(Δ)
N.Tau
S.iAqr
mean shower meteoroid
Quad
αCap
Dra
Δ Calculated Point - No Adjustment
Calculated Point - Efficiency Correction Applied
Calculated Point for mean meteoroid parameters
Observed Temperature Ratio (without error bars)
20
30
40
50
60
70
Geocentric Velocity (Km/sec)

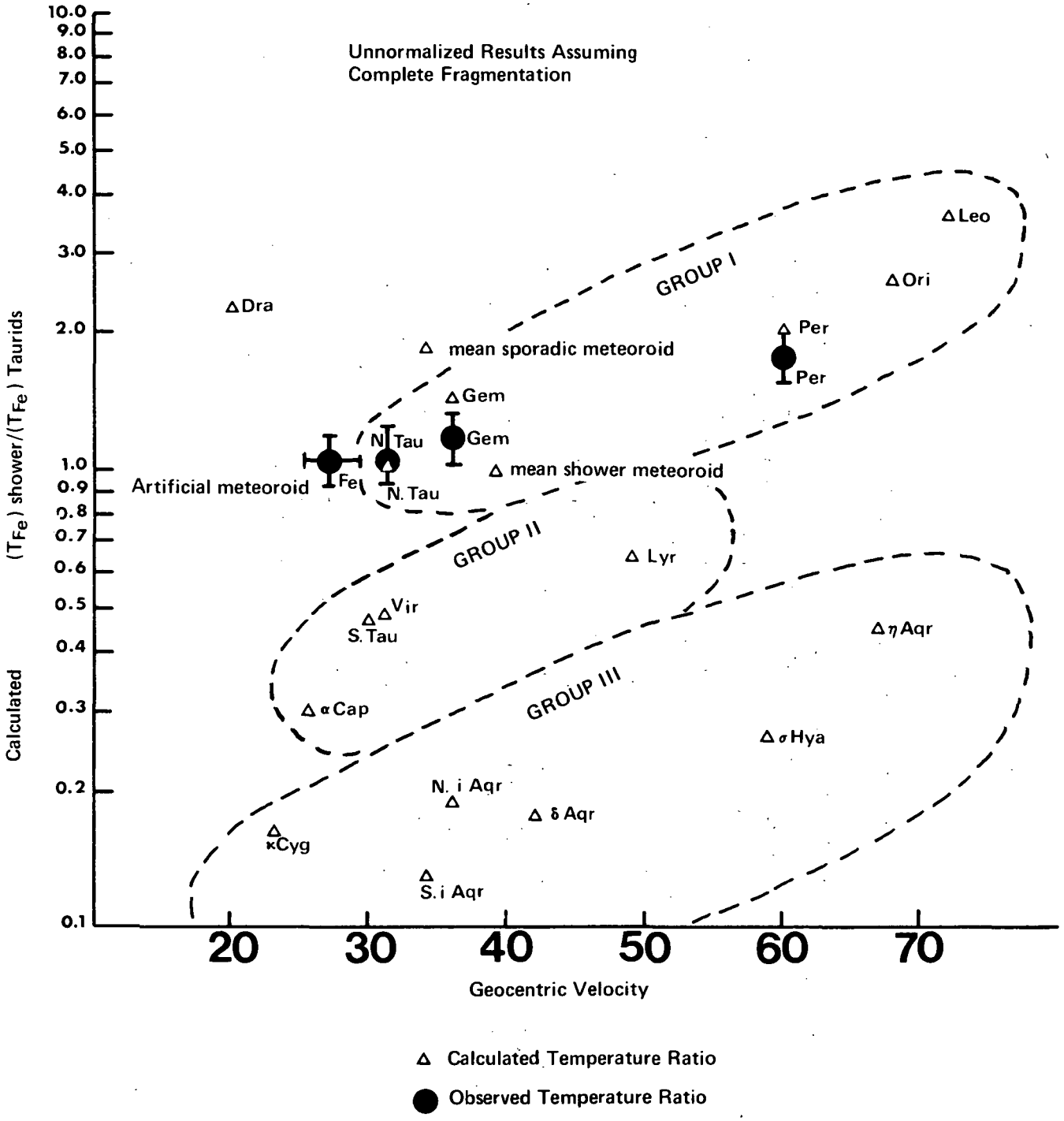
Unnormalized Results Assuming
Complete Fragmentation
Calculated (TFe) shower/(TFe) Taurids
10.0
9.0
8.0
7.0
6.0
5.0
4.0
3.0
2.0
1.0
0.9
0.8
0.7
0.6
0.5
0.4
0.3
0.2
0.1
20
30
40
50
60
70
Geocentric Velocity
GROUP I
GROUP II
GROUP III
Δ Leo
Δ Ori
Δ Dra
Δ Per
Per
Δ mean sporadic meteoroid
Δ Gem
Gem
N. Tau
Δ mean shower meteoroid
Artificial meteoroid
Fe
N. Tau
Δ Lyr
Δ Vir
S. Tau
Δ η Aqr
Δ α Cap
Δ σ Hya
N. i Aqr
Δ δ Aqr
Δ κ Cyg
S. i Aqr
Δ Calculated Temperature Ratio
Observed Temperature Ratio

Outline of Possible Ultraviolet Meteor Experiments

Experiment	Equipment	Expected Scientific Results	Location	Advantages	Disadvantages	Relative Cost*	Suggested Priority
Direct Photography	UV transmitting camera with chopping shutter	Statistics of UV meteors - rates, velocities, and magnitudes	Groundbased above 3 km	Can be automated Use existing facilities and state-of-art equipment	Requires long patrol time subject to weather and moonlight $\lambda \geq 3000$ Å	Low	Low
			Aircraft above 10 km	Uses state-of-art equipment above weather, less extinction	Limited to short duration showers Needs windows, platform $\lambda > 2800$ Å	Moderate to high	Low
			Spacecraft above 150 km	Enables detection down to $\lambda \approx 1000$ Å Not limited by moonlight	If film is used, will require retrieval	High	Low
Broadband Photometry	Multichannel photoelectric photometers with filters	Ultraviolet luminous efficiencies, color index measurements, and light curves	Groundbased above 3 km	Can be automated relatively easily	Does not give direct identification of events $\lambda > 3000$ Å Also moonlight and weather interference	Low	Low
			Aircraft above 10 km	Above weather, less extinction, does not require stabilized platform	Needs special windows and logistics, moonlight sensitive $\lambda > 2800$ Å	Low to Moderate	Low
			Spacecraft above 150 km	Detection to $\lambda \approx 1000$ Å Not limited by weather or moonlight	Problem with event verification	Moderate to high	Low

*Includes transportation

Outline of Possible Ultraviolet Meteor Experiments
(continued)

Experiment	Equipment	Expected Scientific Results	Location	Advantages	Disadvantages	Relative Cost*	Suggested Priority
Narrowband Photometry	Multichannel photoelectric photometers with interference filters	Studies of isolated spectral features and their time histories Abundances can be derived if ionization and identification problems can be worked out.	Groundbased above 3 km	Can be automated and use existing facilities	Problem with event and spectral identification $\lambda \geq 3000$ Å	Low	Moderate
			Aircraft above 10 km	Relatively easy to operate, less extinction, does not need stabilization	Needs special windows and logistics, moonlight sensitive $\lambda \geq 2800$ Å	Low to Moderate	Moderate
			Spacecraft above 150 km	Detection to $\lambda \approx 1000$ Å Not limited by weather or moonlight	Problem with event and spectral identification	Moderate	Moderate
Objective Element Spectroscopy	UV optics on camera with photographic detector and rotating shutter	Better understanding of meteor processes Confirmation and identification of spectral features	Groundbased above 3 km	Relatively simple using state-of-art equipment, event derived	Limited to $\lambda \geq 3000$ Å Sensitive to weather and moonlight	Low	High
			Aircraft above 10 km	Good event and spectral identification, not weather sensitive	Limited to $\lambda \geq 2800$ Å Sensitive to moonlight, requires windows and stable platform	Moderate to High	High
			Spacecraft above 150 km	Detection to $\lambda \approx 1000$ Å Not limited by weather or moonlight	Needs retrieval and further data reduction	Moderate	High
	UV optics on camera with electronographic or electron intensification detector and rotating shutter or equivalent	Direct solution of ionization and dissociation depletion Detailed analysis of elemental abundances of a variety of elements	Groundbased above 3 km	Good event identification, high sensitivity	Limited to $\lambda \geq 3000$ Å Sensitive to weather and moonlight	Moderate to High	High if gain of 10 to 10^2 over photographic is achieved

*Includes transportation

Outline of Possible Ultraviolet Meteor Experiments
(continued)

Experiment	Equipment	Expected Scientific Results	Location	Advantages	Disadvantages	Relative Cost*	Suggested Priority
Objective Element Spectroscopy (continued)	see previous page	see previous page	Aircraft above 10 km	High sensitivity, low extinction, not weather sensitive	Limited to $\lambda \geq 2800$ Å Sensitive to moonlight Needs platform and is more complex	High	High if gain of 10 to 10^2 over photographic is achieved
			Spacecraft over 150 km	Detection to $\lambda \simeq 1000$ Å Not moonlight or weather sensitive High sensitivity	Equipment complexity not state-of-art in all respects	High	

*Includes transportation

NATIONAL AERONAUTICS AND SPACE ADMINISTRATION
WASHINGTON, D.C. 20546

OFFICIAL BUSINESS
PENALTY FOR PRIVATE USE $300

SPECIAL FOURTH-CLASS RATE
BOOK

POSTAGE AND FEES PAID
NATIONAL AERONAUTICS AND
SPACE ADMINISTRATION
451

U.S.MAIL

POSTMASTER: If Undeliverable (Section 158 Postal Manual) Do Not Return

"The aeronautical and space activities of the United States shall be conducted so as to contribute . . . to the expansion of human knowledge of phenomena in the atmosphere and space. The Administration shall provide for the widest practicable and appropriate dissemination of information concerning its activities and the results thereof."

—NATIONAL AERONAUTICS AND SPACE ACT OF 1958

NASA SCIENTIFIC AND TECHNICAL PUBLICATIONS

TECHNICAL REPORTS: Scientific and technical information considered important, complete, and a lasting contribution to existing knowledge.

TECHNICAL NOTES: Information less broad in scope but nevertheless of importance as a contribution to existing knowledge.

TECHNICAL MEMORANDUMS: Information receiving limited distribution because of preliminary data, security classification, or other reasons. Also includes conference proceedings with either limited or unlimited distribution.

CONTRACTOR REPORTS: Scientific and technical information generated under a NASA contract or grant and considered an important contribution to existing knowledge.

TECHNICAL TRANSLATIONS: Information published in a foreign language considered to merit NASA distribution in English.

SPECIAL PUBLICATIONS: Information derived from or of value to NASA activities. Publications include final reports of major projects, monographs, data compilations, handbooks, sourcebooks, and special bibliographies.

TECHNOLOGY UTILIZATION PUBLICATIONS: Information on technology used by NASA that may be of particular interest in commercial and other non-aerospace applications. Publications include Tech Briefs, Technology Utilization Reports and Technology Surveys.

Details on the availability of these publications may be obtained from:

SCIENTIFIC AND TECHNICAL INFORMATION OFFICE

NATIONAL AERONAUTICS AND SPACE ADMINISTRATION

Washington, D.C. 20546